ABSTRACT

Title of Thesis: NIGHTTIME PHOTOVOLTAIC CELLS: ELECTRICAL POWER GENERATION BY OPTICALLY COUPLING WITH DEEP SPACE

Tristan Deppe, Master of Science, 2019

Thesis Directed By: Professor Jeremy Munday
Department of Electrical and Computer Engineering

Photovoltaics possess significant potential due to the abundance of solar power incident on earth; however, they can only generate electricity during daylight hours. In order to produce electrical power after the sun has set, we consider an alternative photovoltaic concept that uses the earth as a heat source and the night sky as a heat sink, resulting in a "nighttime photovoltaic cell" that employs thermoradiative photovoltaics and radiative cooling to output as much as 10 W/m^2 from ambient radiation. This thesis will discuss the principles of thermoradiative photovoltaics, the theoretical limits of coupling a device with deep space, the potential of advanced radiative cooling techniques to enhance their performance, and a discussion of the practical limits, scalability, and integrability of this nighttime photovoltaic concept.

NIGHTTIME PHOTOVOLTAIC CELLS: ELECTRICAL POWER GENERATION BY OPTICALLY COUPLING WITH DEEP SPACE

by

Tristan Jerome Deppe

Thesis submitted to the Faculty of the Graduate School of the
University of Maryland, College Park, in partial fulfillment
of the requirements for the degree of
Master of Science
2019

Advisory Committee:
Professor Jeremy Munday, Chair
Professor Agis Iliadis, co-Chair
Professor Lourdes Salamanca-Riba

Acknowledgements

I would first like to thank my family, friends, and past acquaintances for being a perpetual source of strength, support, and advice throughout my life and career. Secondly, I have to express my sincere gratitude for my undergraduate professors, Dr. Paola Barbara, Dr. Mak Paranjape, and Dr. Peter Pfeiffer, and former colleagues, Dr. Mary Galvin and Dr. Linda Sapochak, whose mentorship and perpetual willingness to write last-minute letters of recommendations have allowed me to have such a diverse and rewarding career, both inside and out of academia. I must next recognize my graduate advisor, Dr. Jeremy Munday, who served as a source of direction throughout my work, and all my present and former colleagues in the Munday Lab and in IREAP, notably Kevin Palm, Joe Murray, Joe Garrett, Lisa Krayer, David Somers, Sarvenaz Memarzadeh, Jongbum Kim and John Howard, for their patience and assistance, especially in the early stages of my studies and research. Finally I wish to thank the staff in IREAP and the ECE department for their kindness, which helped make these past two years at University of Maryland an enjoyable and welcoming experience.

Table of Contents

List of Tables

List of Figures

List of Abbreviations and Symbols

ATW	Atmospheric Transparency Window
IR	Infrared
LWIR	Long-wave Infrared Radiation
PMMA	Polymethyl Methacrylate
PV	Photovoltaic
PVF	Polyvinyl Fluoride
Si	Silicon
TPX	Polymethyl Pentene
TR	Thermoradiative
UV	Ultraviolet

c	Speed of Light
ε	Emissivity
E	Energy (of a Photon)
E_g	Bandgap
eV	Electronvolt
h	Planck's Constant
I	Current
K	Degrees Kelvin
k_B	Boltzmann's Constant
n	Electron (Density)
n_o	Intrinsic Electron Concentration
n_i	Intrinsic Carrier Concentration
p	Hole (Density)
p_o	Intrinsic Hole Concentration
P	Power
q	Electron Charge
Q	Heat
R	Reflectivity
T	Temperature
V	Voltage
W	Work
μm	Micron (1×10^{-6} m)
$\Delta\mu$	Chemical Potential

List of Publications

Portions of this thesis have been drawn from the following publication:

Tristan Deppe and Jeremy N. Munday. Nighttime Photovoltaic Cells: Electrical Power Generation by Optically Coupling with Deep Space. *ACS Photonics* 2020, *7***,** 1, 1-9.

Chapter 1: Introduction

Currently over 100 US cities have committed to using 100% clean, renewable electricity by 2050, and solar energy is expected to help supply the needed additional power. However, conventional photovoltaic (PV) cells can only generate electricity during daylight hours, while energy consumption peaks in the evening. This lack of nighttime performance necessitates the need for costly batteries to store solar-generated power and grid connection to other sources of energy, most notably fossil fuels. To continue the global push towards carbon neutrality, new sustainable power generation techniques must be employed at night as well. The work of this thesis proposes and explores an alternative PV concept that employs thermoradiative cells and the advancing field of radiative cooling in order to generate electrical power during the day and throughout the night. This first section includes an introduction to the fields that have inspired this work and an overview of the analysis and results.

1.1 How would a nighttime photovoltaic cell work?

Though the power conversion process of a solar cell is governed by the principle of detailed balance,[1] it can also be modeled as a simplified heat engine. Ultimately the cell delivers power because the radiation source, the sun, is very hot, and the solar cell, in comparison, is cool (Figure 1.1a). Alternatively, we can heat up the solar cell, which becomes the hot object, and point it at a cold object, e.g. the night sky (Figure 1.1b). In both cases we have one hot object and one cold object, and we can study the power flow between them. In the second case, this type of heat engine is called a

thermoradiative (TR) cell.[2] Explained in detail in Chapter 2, a TR cell generates power because the emission of thermal radiation from the cell exceeds the absorption of irradiation from the surroundings during operation. The actual devices, a solar cell and a TR cell, are nearly identical, however the operating currents and voltages have opposite signs because the radiative processes are reciprocal (Figure 1.2). In practice, TR cells can be used as waste heat recovery units in order to extract power from a hot source, e.g. an engine's exhaust pipe, a generator's cooling towers, or other sources in industrial manufacturing plants. The cell simply needs to be at a higher temperature than the object towards which it radiates. The nighttime PV cell concept relies on the thermoradiative effect and uses the warmth of the earth, at about 300 K, as a heat source and the darkness of space, at 3 K, as a heat sink. The key to making this concept work is then two-fold. Firstly, we must choose a material with the appropriate bandgap needed to maximize power output. Secondly, the device must be able to "see" through the atmosphere in order to optically couple with space.

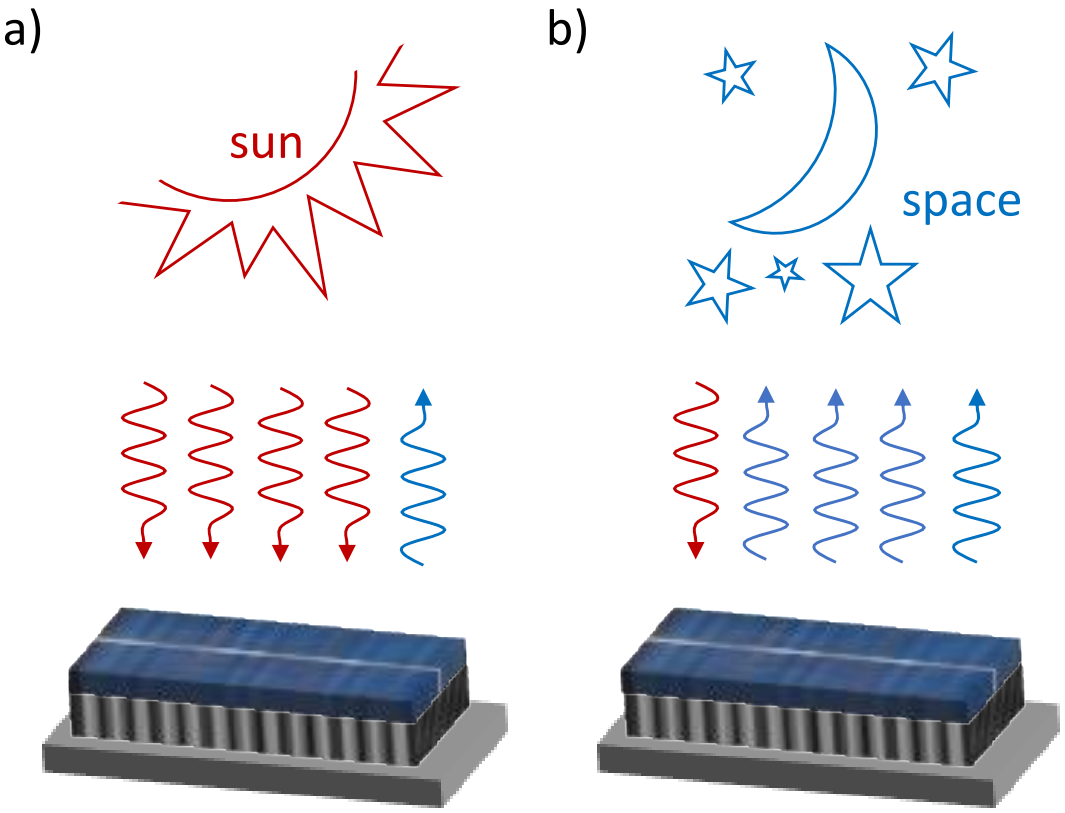

Figure 1.1 (a) A photovoltaic cell illuminated by solar irradiation during the day. Absorbed photons create electron-hole pairs across the semiconductor bandgap and establish a working voltage, *V*. (b) A thermoradiative cell at night. The cell emits thermal radiation in the infrared into space. As electron-hole pairs recombine across the semiconductor bandgap, a negative voltage is established. Tristan Deppe and Jeremy N. Munday. Nighttime Photovoltaic Cells: Electrical Power Generation by Optically Coupling with Deep Space. *ACS Photonics* 2020, *7***,** 1, 1-9.

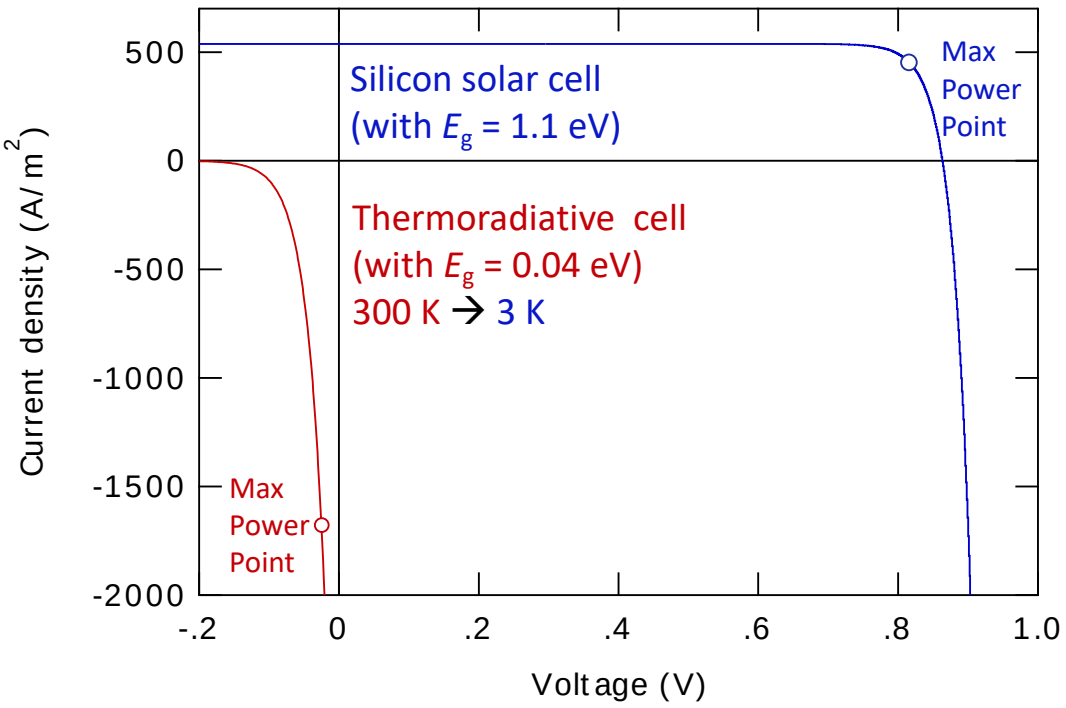

Figure 1.2 *I-V* characteristics of a photovoltaic (quadrant 1) and an ideal thermoradiative (quadrant 3) cell of bandgap 1.1 eV and 0.04 eV, respectively, both show power generation. For the thermoradiative cell, negative voltage and negative current generate positive power across an external load. Tristan Deppe and Jeremy N. Munday. Nighttime Photovoltaic Cells: Electrical Power Generation by Optically Coupling with Deep Space. *ACS Photonics* 2020, *7***,** 1, 1-9.

1.2 Potential

A typical single junction solar cell is made from a semiconductor with a bandgap in the range of 1.0 to 1.5 eV. Most modern commercial cells operate at approximately 20% efficiency and are made of silicon, with a 1.1 eV bandgap, yielding approximately 200 W/m^2 under peak solar irradiance (~1000 W/m^2). If silicon were used for a nighttime PV cell, the principles of detailed balance, outlined in the following section, lead to a maximum power output of < 2 x 10^{-14} W/m^2. This result is because the vast majority photons emitted by a blackbody near room temperature are

infrared, with energy far less than the bandgap of silicon (Figure 1.3). However, if an ultralow-bandgap material were used to make a device, low energy photon emission results from carrier recombination across the gap and, when connected to a load, an ideal cell could produce as much as 54 W/m^2 in optimal conditions and potentially more than 10 W/m^2 under typical sky conditions, both to be discussed later, without the need for solar absorption. Though this power output is lower than a conventional solar cell, it could be produced day and night. Further, one can envision a tandem system consisting of a TR device operating at night and a standard solar cell operating during the day to produce higher total around-the-clock power. For example, in an average US climate, such as Boulder, CO, the National Renewable Energy Laboratory database records an average solar irradiance of about 5 kWh/m^2 per day,[3] of which a commercial solar cell could harvest 1 kWh/m^2. A nighttime PV cell in this climate could produce an average of 120 Wh/m^2 (if operated during only 12 hours), thus adding ~12% more power to the 24-hour cycle.

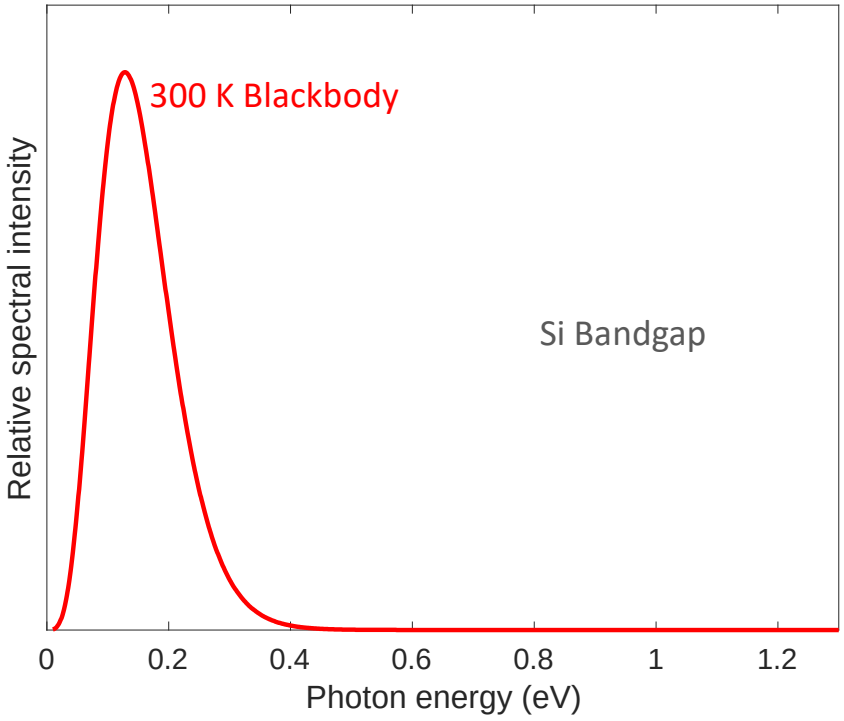

Figure 1.3 Relative spectral intensity with respect to photon energy, in eV, for a 300 K blackbody emitter. The emitted photons are much lower energy than the bandgap of Si, at 1.1 eV. To extract useful power from an emitter at 300 K, a material with energy gap around the peak of the emission spectrum, between 0 and 0.2 eV, must be used.

1.3 Optically coupling to space

To directly access deep space as a thermal reservoir, we next consider the topic of radiative cooling. For millennia humans have understood that material choice and architectural design can heat or cool structures above or below ambient air temperature.[4] Today, white paint is sometimes used to coat the roofs of buildings in order to reflect sunlight and thereby reduce heating during the day. In recent years, however, the study of radiative cooling has garnered attention with the development of highly thermally emissive, yet solar reflective materials, that can be used to lower an object's surface temperature significantly below ambient.[5-8] A similar technique can

also be extended to traditional solar cells to avoid heating during operation and thus increase device efficiency.[9,10] By appending a photonic material that is visibly transparent, yet thermally emissive within the atmospheric transparency window of 8 - 13 μm, solar radiation is still delivered to the cell to generate power, but thermal heat is radiatively exhausted to deep space. These concepts inspire the engineering of a nighttime PV cell in order to extract electrical power from the radiative emission of thermal wavelengths from a device on earth to outer space.

1.4 Outline of thesis

We will first discuss the background and history of thermoradiative photovoltaics (TR PV) in Chapter 2 and the use of selectively emissive materials in cooling applications in Chapter 3. Chapter 4 will then discuss the fundamental limits of the proposed nighttime photovoltaic cell. We introduce a simple model for a TR PV device that generates power by using the heat of the earth as a thermal power source and the night sky as a thermal radiative heat sink. We then calculate the fundamental limits of such a device. In Chapter 5 we discuss possible materials, their respective practical limits, and finally the scalability, integrability, and energy harvesting potential of a nighttime PV cell. Chapter 6 concludes the work with a discussion of the impact of the study and the work needed to further the technology.

a)

Figure 1.4a Cartoon representation of Figure 1.1a, a photovoltaic cell illuminated by solar irradiation during the day. Absorbed photons create electron-hole pairs across the semiconductor bandgap and establish a working voltage, *V*. Tristan Deppe and Jeremy N. Munday. Nighttime Photovoltaic Cells: Electrical Power Generation by Optically Coupling with Deep Space. *ACS Photonics* 2020, *7***,** 1, 1-9.

b)

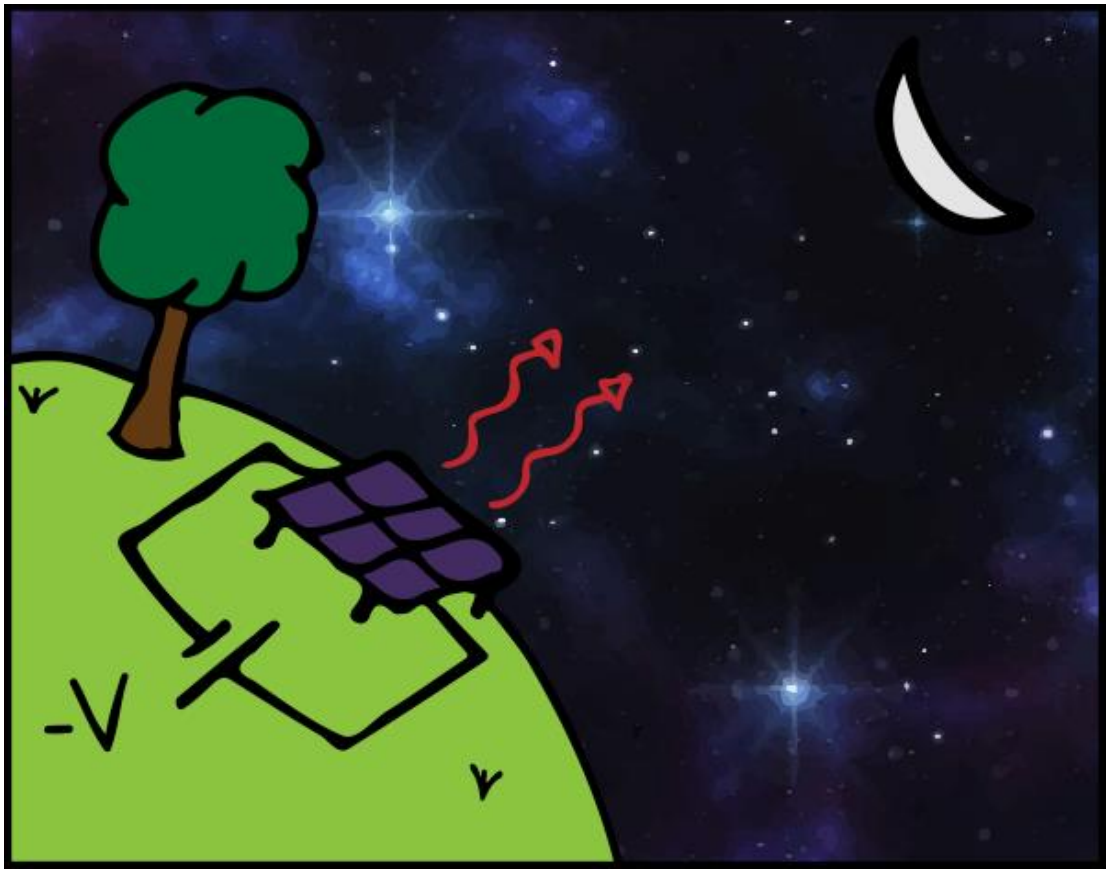

Figure 1.4b Cartoon representation of Figure 1.1b, a thermoradiative cell at night. The cell emits thermal radiation in the infrared into space. As electron-hole pairs recombine across the semiconductor bandgap, a negative voltage is established. Image selected for cover of January issue of ACS Photonics. Tristan Deppe and Jeremy N. Munday. Nighttime Photovoltaic Cells: Electrical Power Generation by Optically Coupling with Deep Space. *ACS Photonics* 2020, *7***,** 1, 1-9.

Chapter 2: Thermoradiative Photovoltaics

In this chapter, we will present the physical principles that govern thermoradiative photovoltaics, the driving mechanism behind a nighttime photovoltaic cell. We explain the electron transport within such a device, correlating it to a standard photovoltaic cell, and introduce the equations used to calculate power. We then discuss efficiency and conclude with an overview of previous work.

2.1 Physical principles

The physical principles governing TR cells are similar to those behind conventional photovoltaics.[2,11-14] When a *p*-*n* junction is in thermal equilibrium with its surroundings in the dark (Figure 2.1a), the random absorption of photons by the cell equals the random emission from the cell, and the Fermi level remains constant throughout the semiconductor. Under illumination and normal PV cell operation (Figure 2.1b), absorption is greater than emission, and this difference generates photocurrent. Photon absorption increases the total electron and hole carrier density, which increases the quantity np to greater than $n_o p_o = n_i^2$, the square of the total intrinsic carrier density. This excess carrier generation splits the electron and hole Fermi levels within the junction by an amount $\Delta\mu = qV$, which are then referred to as the quasi-Fermi levels. If the cell is connected to a load, excess electrons and holes that do not recombine within the material can be extracted on the *n*- and *p*-side, respectively, with energy slightly below qV due to thermodynamic losses. If the *p*-*n* junction is at a higher temperature than its surroundings (Figure 2.1c), emission from the device dominates absorption as the device tries to cool. However, if the cell is connected to a thermal

reservoir, its temperature remains constant. In this case, the enhanced emission decreases the carrier concentration below its equilibrium value, $n_o p_o$, which splits the electron and hole Fermi levels in the opposite direction and introduces a reverse bias voltage across the junction. When short-circuited or connected to a load, the recombination of an electron and hole pair that is not balanced by absorption of a photon results in an additional electron and hole being inserted via the contacts to balance the lost pair. This injection results in current flow. Functionally, the main difference between a TR PV cell and a conventional PV cell is that (i) the current flows in the opposite direction and (ii) the sign of the voltage is also reversed; therefore, both scenarios generate usable power.

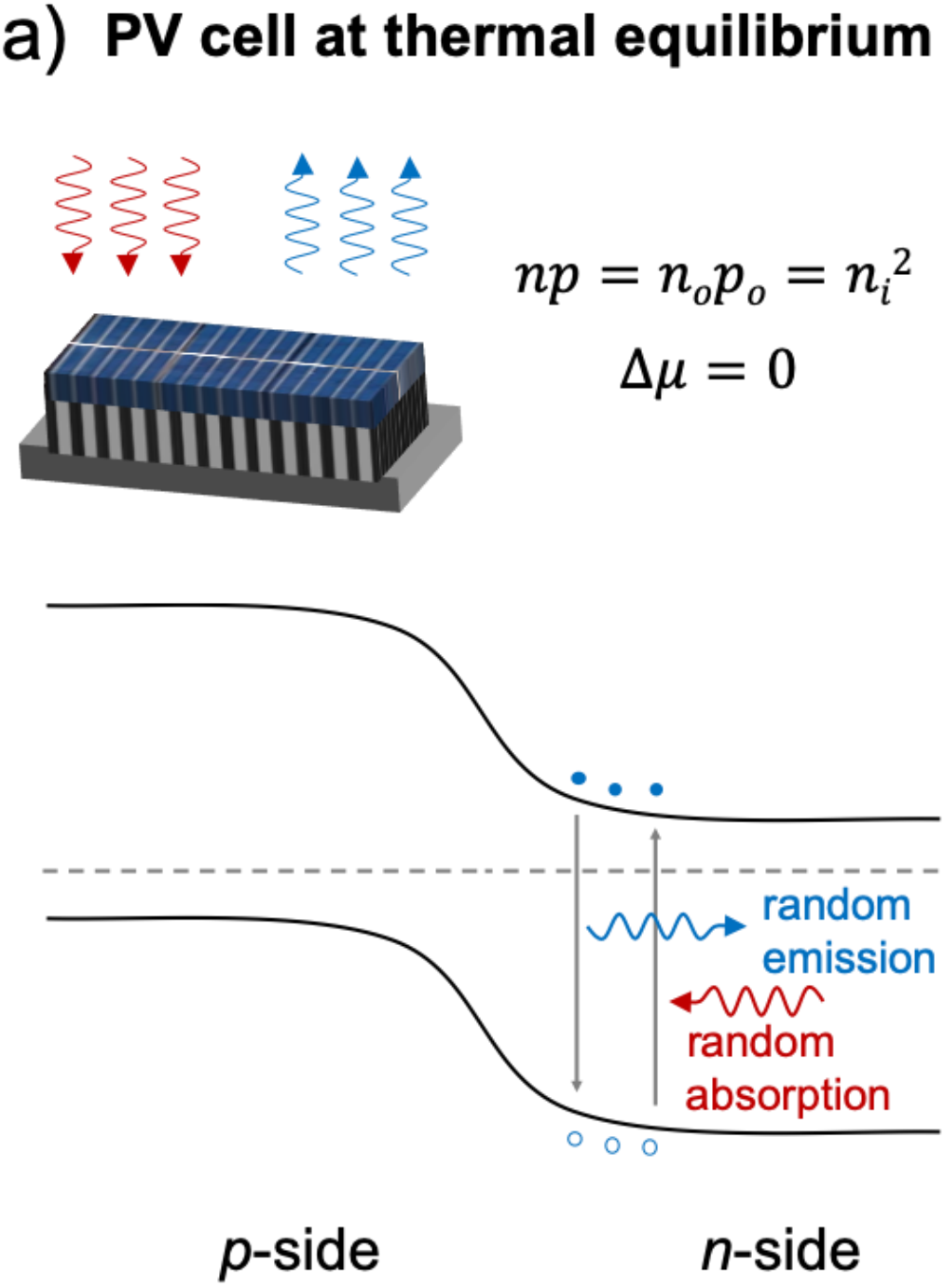

Figure 2.1a Band diagram and the path of carriers through a *p-n* junction at thermal equilibrium, where emission balances absorption and no current is produced. Tristan Deppe and Jeremy N. Munday. Nighttime Photovoltaic Cells: Electrical Power Generation by Optically Coupling with Deep Space. *ACS Photonics* 2020, *7***,** 1, 1-9.

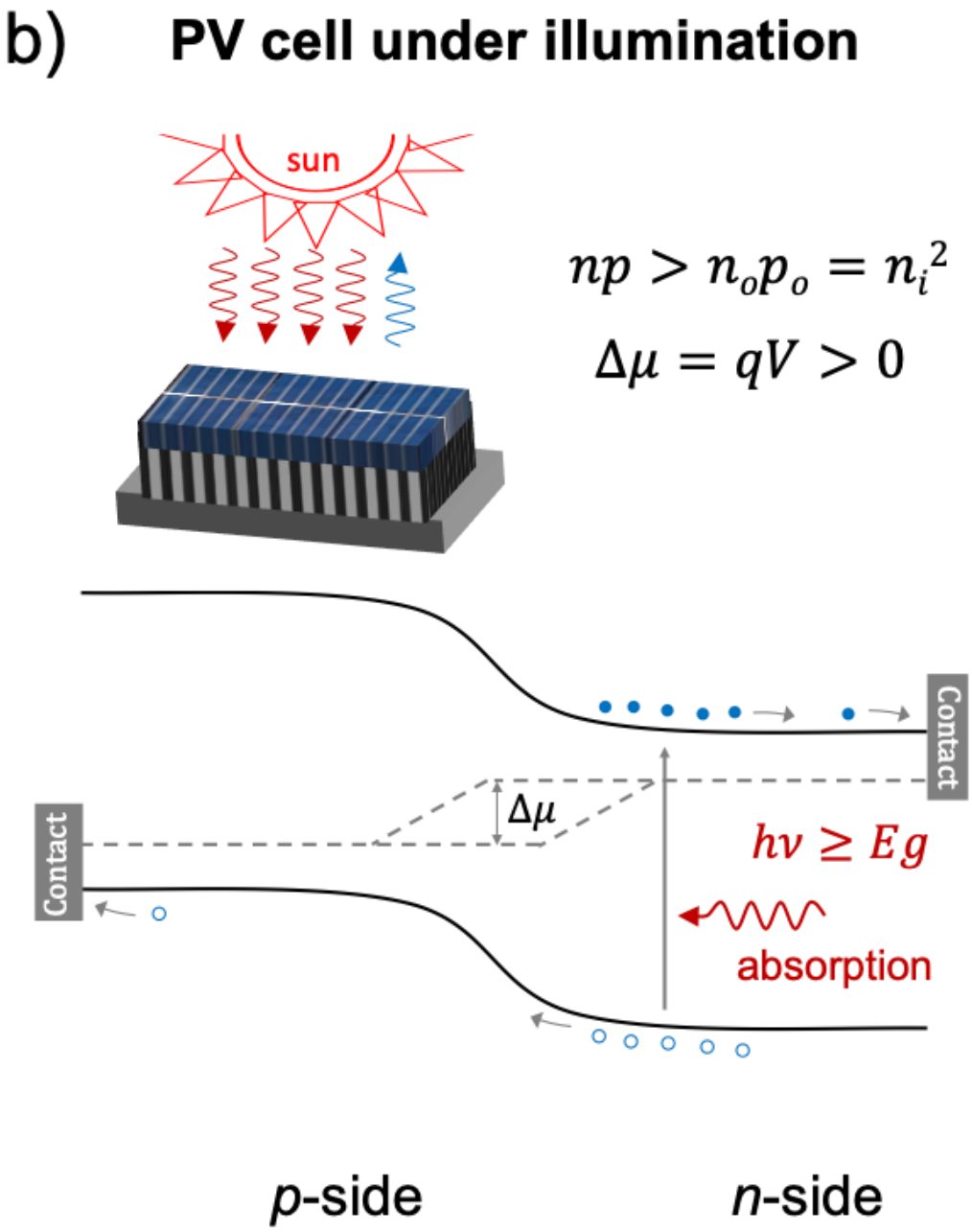

Figure 2.1b A *p-n* junction under illumination, i.e. conventional solar cell operation, where excess carriers are created due to absorption and extracted at the contacts when connected across an external circuit. Tristan Deppe and Jeremy N. Munday. Nighttime Photovoltaic Cells: Electrical Power Generation by Optically Coupling with Deep Space. *ACS Photonics* 2020, *7***,** 1, 1-9.

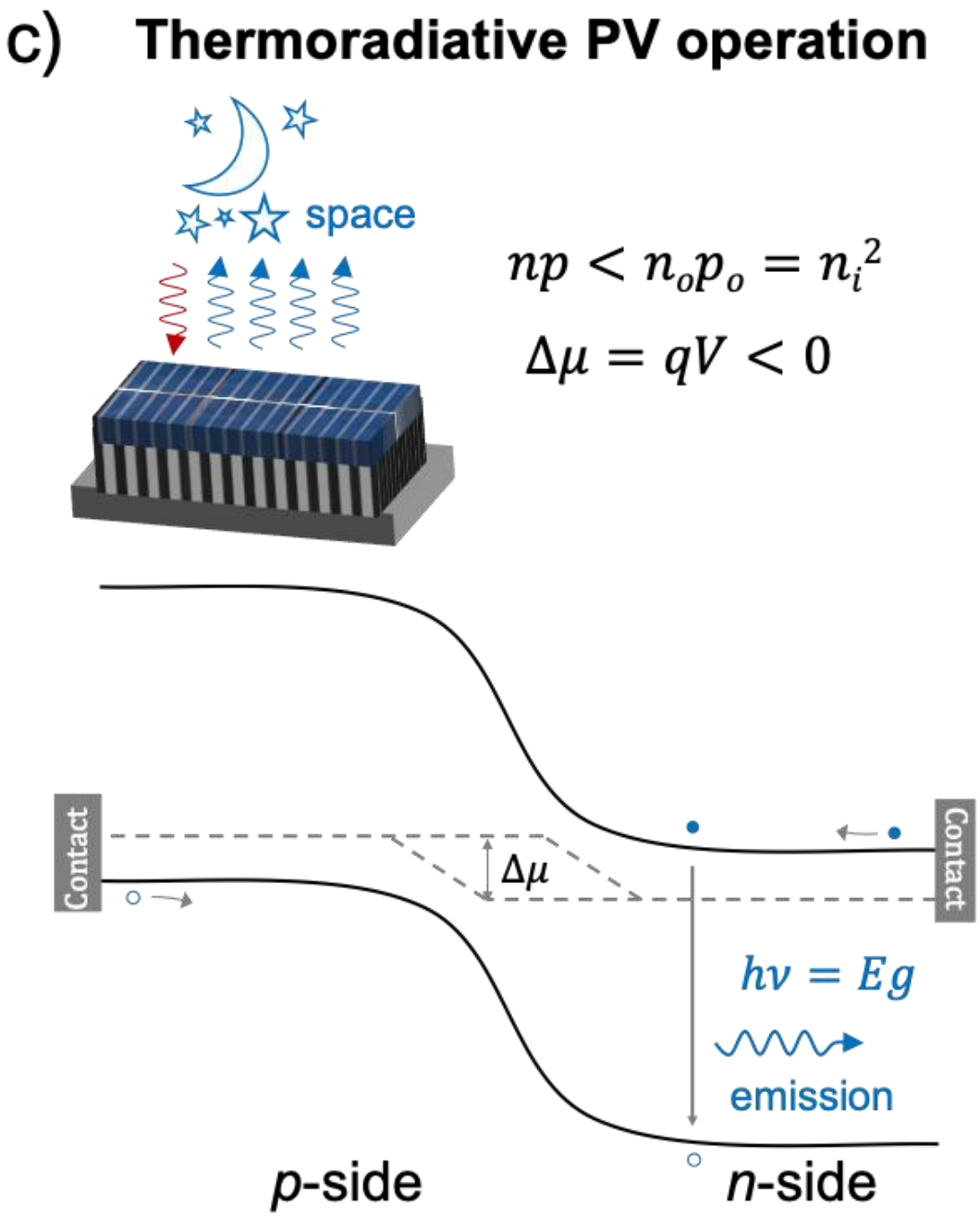

Figure 2.1c A *p-n* junction functioning as a thermoradiative cell, where emission reduces the carrier concentration below thermal equilibrium and a reverse bias forms across the junction. When connected to an external circuit, current flows in the reverse direction as under illumination, and carriers are inserted at the contacts. Tristan Deppe and Jeremy N. Munday. Nighttime Photovoltaic Cells: Electrical Power Generation by Optically Coupling with Deep Space. *ACS Photonics* 2020, *7***,** 1, 1-9.

2.2 Mathematical analysis

To describe the current and power produced by a TR cell at temperature T_c exposed to a cooler body at temperature T_a, we use the principles of detailed balance, formulated by Shockley and Queisser. First, the photon flux emitted from an illuminated or biased semiconductor is derived from Planck's generalized law for blackbody radiation and is equal to[15]

$$\dot{N}(T, \Delta\mu) = \frac{2\pi}{h^3 c^2} \int_{E_g}^{\infty} \frac{\varepsilon(E) E^2}{e^{\frac{E-\Delta\mu}{k_B T}} - 1} dE, \tag{2.1}$$

where T, $\Delta\mu$, $\varepsilon(E)$, and E_g are the temperature, the chemical potential driving emission, the energy-dependent emissivity, and the bandgap of the semiconductor, respectively, while h is Planck's constant, k_B is Boltzmann's constant, c is the speed of light, and the integral is taken over photon energy, E. In the absence of non-radiative recombination, the external current produced by the cell must equal the difference between photon absorption and photon emission. Illuminated by a radiative body at T_a, an ideal cell at temperature T_c will produce a current density through an external circuit equal to

$$J = q\left[\dot{N}(T_a, 0) - \dot{N}(T_c, \Delta\mu_c)\right], \tag{2.2}$$

where $\Delta\mu_c$ is the cell's chemical potential, which is equal to the quasi-Fermi level splitting and is related to the output voltage by $\Delta\mu_c = qV$. As mentioned above, in a TR cell emission dominates absorption, as $T_c > T_a$. For a cell that is a perfect emitter and absorber of photons at or above the bandgap energy of the semiconductor and is transparent to lower energy photons (i.e. ε=0 for E<E_g, and ε=1 for $E \geq E_g$), one can

see from eqs 2.1 and 2.2 that the current will be negative. By attaching a load across the cell, the extractable power density is

$$P = JV = qV\left[\dot{N}(T_a, 0) - \dot{N}(T_c, qV)\right]. \tag{2.3}$$

2.3 The matter of efficiency

The efficiency of a TR cell has been derived for cases where the device is heated up to temperatures above ambient[2,12] and when emission is restricted to a very narrow bandwidth.[13,14] In these situations, the cell is exchanging energy with its ambient environment, e.g. a hot cell in a cold room, which functions as a heat sink. This scenario is modeled thermodynamically as a heat engine in Figure 2.2.

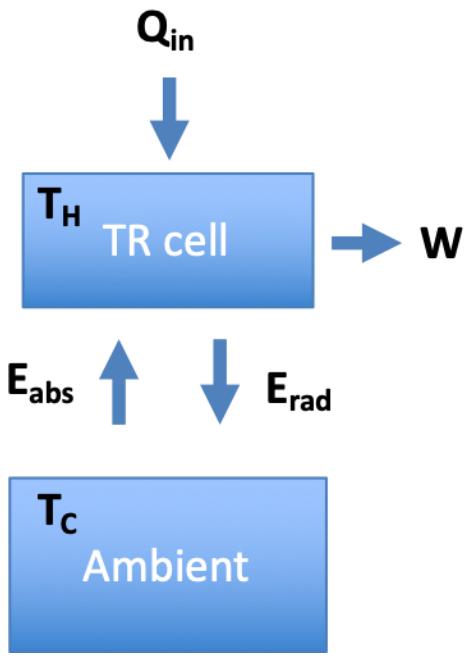

Figure 2.2 A thermodynamic model of a TR cell exchanging energy with its environment. The TR cell is held at a higher temperature than the ambient due to some heat input mechanism, Q_{in}. Energy is exchanged between the two blackbodies, i.e. E_{rad} is emitted from the cell to the ambient, and E_{abs} is emitted from the ambient and absorbed by the cell. The cell is at the higher temperature, as $T_H > T_C$, therefore $E_{rad} > E_{abs}$, and work, W, can be extracted from the cell.

Through a radiative exchange with the environment, the cell absorbs and emits energies E_{abs} and E_{rad}, respectively. If the cell is hotter than the ambient, such that $T_H > T_C$, electrical power can be produced by the cell in the form of work, W. Following Strandberg's treatment for a steady-state case,[2] where T_H and T_C remain constant, the total energy flowing into the cell must equal the energy flowing out, such that

$$Q_{in} + E_{abs} = W + E_{rad} . \tag{2.4}$$

If we consider the traditional efficiency,

$$\eta = P_{out}/P_{in} , \tag{2.5}$$

P_{in} can be defined as Q_{in}, the heat added to the cell to maintain a constant cell temperature, T_H, above the ambient temperature, T_C. P_{out} is the electrical power, W, extracted from the system. With this formulation, we can solve equation 2.4 for Q_{in}, input it into 2.5, and follow the principles of detailed balance using equations 2.1 and 2.3 to find the efficiency of a thermoradiative cell at various temperatures within an ambient environment of T_C = 300 K. Figure 2.3 shows the efficiency as a function of operating voltage for a 500 K cell, at various bandgap energies, in a 300 K ambient. Table 2.1 shows the maximum efficiency and maximum extractable power. One notes that maximum power is extracted at lower operating voltages while maximum efficiency is obtained with higher voltage.

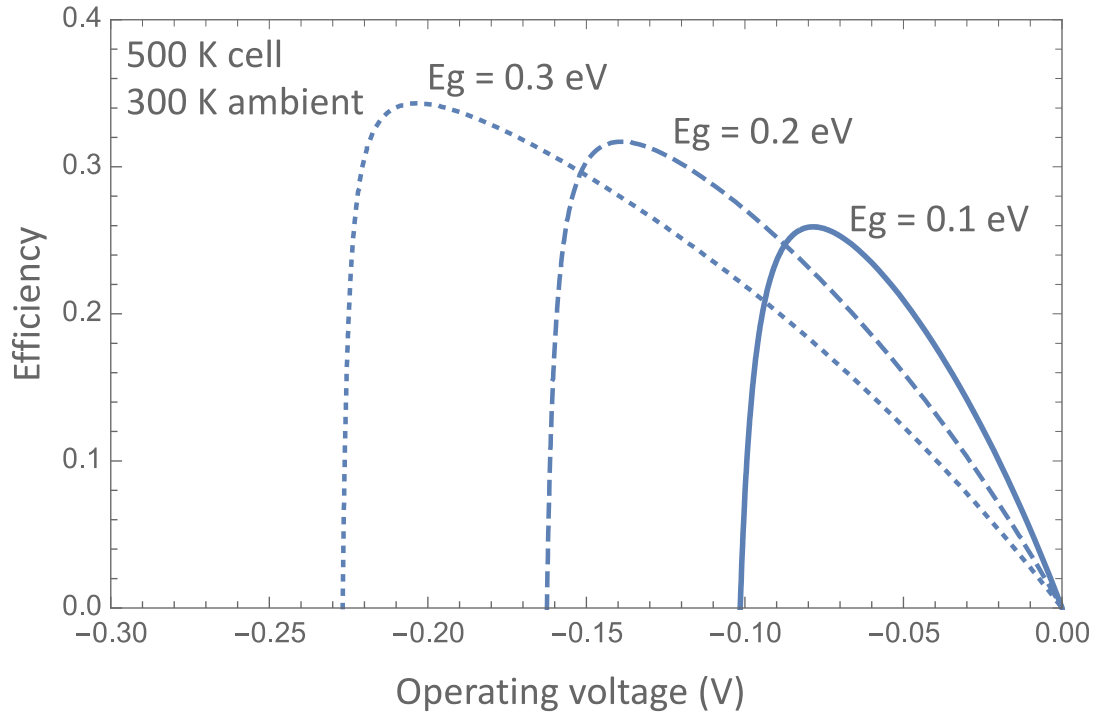

Figure 2.3 Efficiency as a function of operating voltage for a thermoradiative cell held by some external heat source at 500 K within a constant 300 K environment. The maximum extractable powers are 186, 59.8, and 12.1 W/m^2 for bandgap energies of 0.1, 0.2 and 0.3 eV, respectively, as seen in Table 2.1.

Eg (eV)	MEP (V)	Eff (%)	MPP (V)	Pow (W/m^2)
0.3 eV	-0.20	34	-0.042	12.1
0.2 eV	-0.14	32	-0.040	59.8
0.1 eV	-0.08	26	-0.038	186

Table 2.1 The maximum efficiency point (MEP) and maximum power point (MPP) are the operating voltages at which the maximum efficiency and maximum power can be extracted from the cell. The table shows these max values with their corresponding operating voltages for various material energy gaps for a thermoradiative cell at 500 K radiatively coupled to a 300 K ambient environment.

2.4 Direction of this work

Unlike the scenario described in the previous section, in our configuration for a nighttime photovoltaic device, the cell is maintained at ambient temperature by the earth, rather than heated above ambient temperature by an external heat source, and is optically coupled with space as its heat sink. Because no work is done to heat the cell (noting that it is connected to an effectively infinite thermal reservoir), the traditional efficiency, P_{out}/P_{in}, becomes a less useful metric as P_{in} is simply conductive sources of heat from the earth and the surroundings plus the ambient radiation into the cell. A plot of the efficiency, following the treatment outlined in the previous section, can be found in Appendix B, however, the purpose of this thesis is to analyze the extractable electrical power per unit area rather than the efficiency of such a process.

Low bandgap materials are needed for TR devices so that the bandgap energy more closely matches the peak of the device's thermal emission spectrum, as shown previously in Figure 1.3. In the discussion in Chapter 4, we focus on the potential to extract power from a cell around ambient temperature, T_c = 300 K, using the Earth as a heat source and the night sky, which also varies in temperature, as a heat sink, as illustrated previously in Figures 1.1b and 1.4b. Recently, Santhanam and Fan showed that a HgCdZnTe thermoradiative cell (with E_g = 0.218 eV) could deliver 1 pW of power when held at 295 K and exposed to an emissive plate with a 10 K temperature difference.[14] To enhance the extractable power past the pW scale, in the following chapter, we consider ideas from the advancing field of radiative cooling to employ deep space as a heat sink to allow for a significantly larger temperature difference and increase power production.

Chapter 3: Radiative cooling

For a thermoradiative cell to generate power, as outlined in the previous chapter, the photon flux out of the cell must be greater than the photon flux into the cell. Since the nighttime photovoltaic cell is held at ambient temperature and uses space as a heat sink, the top surface of the nighttime photovoltaic cell must be optically coupled with the night sky. The following chapter serves as a review of materials that have been designed to enable this behavior within the field of radiative cooling.

3.1 Key factors in radiative cooling

The key factors needed for effective daytime radiative cooling are:

(i) the ability to transmit or reflect solar illumination to avoid heating,

(ii) thermal isolation from the environment to limit additional conductive and convective heat exchanges with the surroundings, and

(iii) the ability to emit wavelengths that fall within the atmospheric transparency window to enable radiative heat transfer to deep space.

While earth's atmosphere absorbs and reflects at various wavelengths, there is a region within the infrared portion of the electromagnetic spectrum for which the atmosphere is mostly transparent. This is known as the atmospheric transparency window (ATW) and falls roughly between 8 – 13 μm (Figure 3.1). Note there is also a secondary window at slightly longer wavelengths.

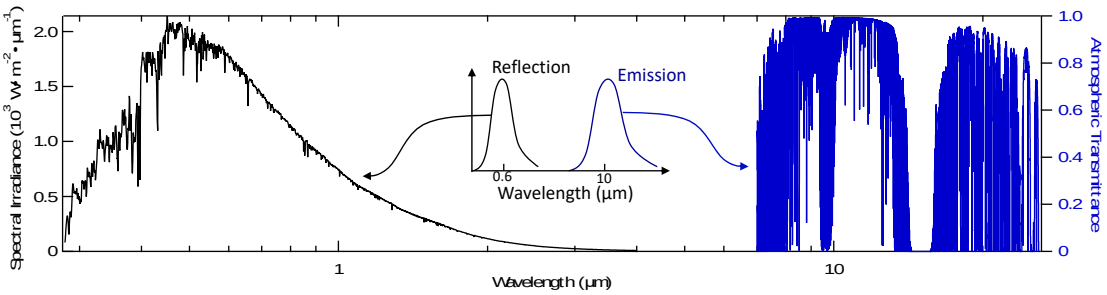

Figure 3.1 The majority of the solar irradiance incident on earth (left) falls in the visible range of the electromagnetic spectrum, compared to the transmittance spectrum of the atmosphere (right), of which the portion between 8 and 13 μm is known as the atmospheric transparency window (ATW). This is the spectral region through which thermal radiation can escape the atmosphere. The insert shows the simplified spectral characteristics of a radiative cooler that reflects the solar wavelengths and emits within the ATW. Solar data from nrel.gov and atmospheric data from gemini.edu. Tristan Deppe and Jeremy N. Munday. Nighttime Photovoltaic Cells: Electrical Power Generation by Optically Coupling with Deep Space. *ACS Photonics* 2020, *7***,** 1, 1-9.

The earth, whose surface temperatures range from about 220 to 320 K, emits strongly within this infrared window, the peak of a 300 K blackbody falling at 9.7 μm or 0.13 eV in Figure 1.3. These long-wave infrared (LWIR) wavelengths can pass through the atmosphere, a phenomenon that allows for the earth to regulate its own temperature and remain habitable. Furthermore, materials that emit and absorb predominately over this bandwidth but reflect or transmit the solar spectrum are optically coupled to deep space but blind to the atmosphere and the sun. Using a material with such a tailored emission spectrum allows for the dramatic cooling of its substrate through photonic emission both at night and under direct sunlight. This concept has also recently been suggested as an additional mitigation strategy to address climate change.[16]

3.2 Traditional and commercial methods

White paints have traditionally been used to achieve this effect on a commercial scale as they can easily be applied over large areas and reflect most of the solar spectrum, with hemispherical solar reflectivity, $R_{solar,}$ up to ~0.94 (over a wavelength range of ~0.3 – 2.5 μm).[17] Many pigments also emit well in the IR, with broadband hemispherical thermal emittance, $\varepsilon_{IR,}$ up to ~0.90 (over a wavelength range of 3 – 25 μm).[17] However, common white pigments like titania and zinc oxide absorb strongly in the UV, which limits cooling performance under direct sunlight.[6,7] Some transparent polymers, such as PMMA,[18] have excellent broadband thermal emittance, while others, like TPX and PVF,[19] emit selectively in the LWIR. Consequently, there are numerous thermoplastic films and membranes available on the market that utilize different combinations of polymers to achieve effective daytime cooling, the best with R_{solar} and ε_{IR} around ~0.90.[17] Like white paints, these polymer-based radiative cooling materials are also easily appended to large areas, either rolled out as singly-ply or composite sheets, or applied in fluid-form to dry as a membrane.

3.3 State of the art

In recent years, likely due to increased global concern about climate change and the corresponding shift in focus towards sustainable energy practices, radiative cooling has garnered a renewed interest in the research community. Accordingly, rapid advancements in radiative cooling have been made to craft different types of photonic metamaterials, many based on the emissive polymers highlighted in the previous section, that can improve on commercially available paints and films.[5-8] The materials

highlighted in Figures 3.2, 3.3, 3.4 and 3.5 are constructed differently yet operate on similar principles, described in Section 3.1. When appended to other surfaces, these materials have been shown to actually reduce substrate temperature below ambient and, in arid environments, are capable of radiating more than 100 W/m^2 night and day.[6,8] Metamaterials based on paint-format SiO_2 microspheres,[7] shown in Figure 3.4, similar to the method characterized by Gentle and Smith,[20] or the porous $P(VdF\text{-}HFP)_{HP}$ coating highlighted in Figure 3.5, with $R_{solar} > 0.96$ and hemispherical LWIR emittance of $\varepsilon_{LWIR} > 0.97$, outperform commercial daytime cooling methods while retaining their scalability.

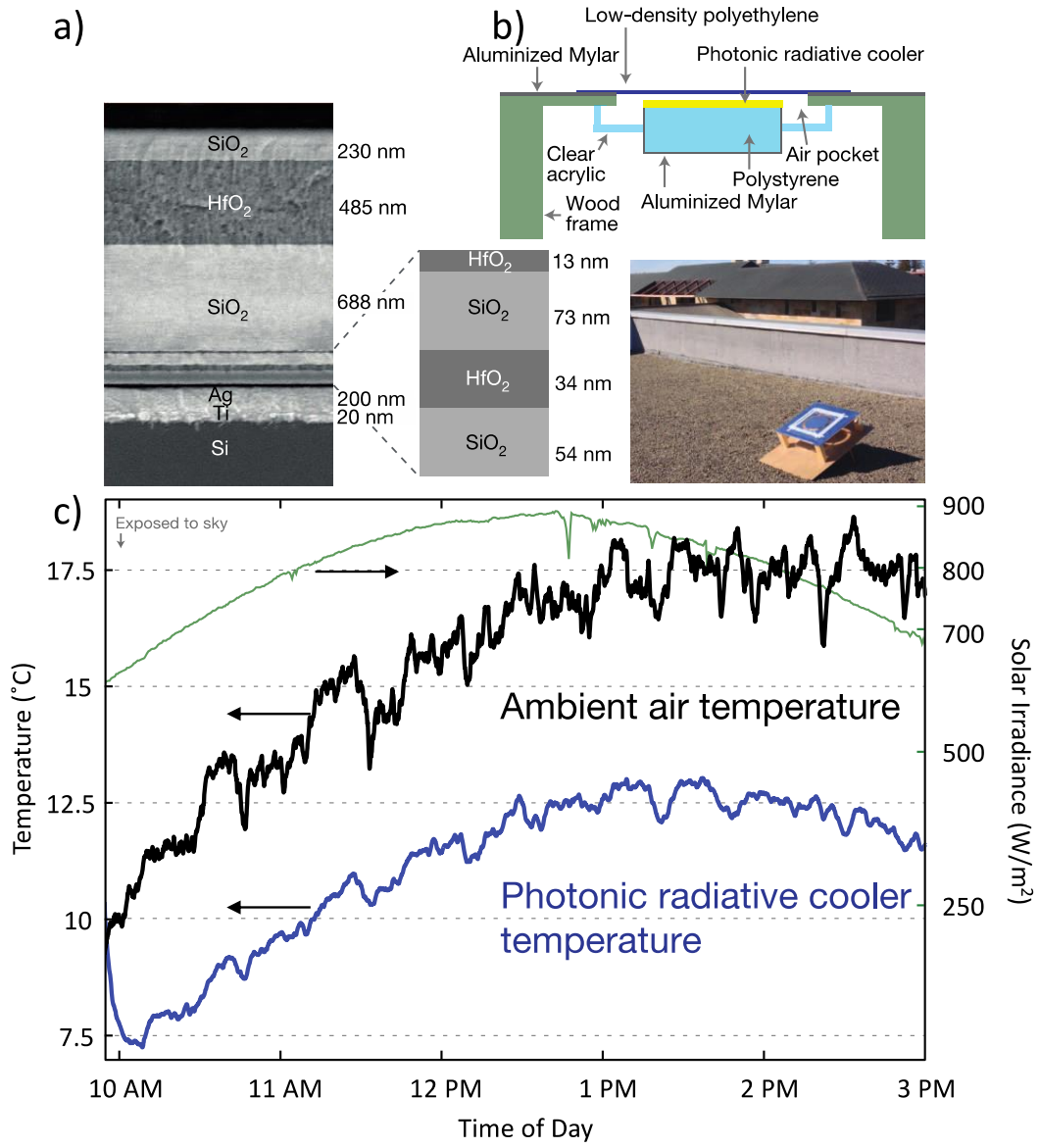

Figure 3.2 By alternating layers of SiO_2 and HfO_2, Raman *et. al.* demonstrated that a combination of material properties and interference effects will produce a photonic radiative cooler that cools to 4.9 K below ambient air temperature under direct sunlight.[5] The structure of the multilayered radiative cooler (a) is shown, next to a schematic of the experimental set-up (b), whose inlay shows a photo of the experiment. The temperature of the radiative cooler is plotted (c) along with the ambient air temperature throughout the day. The right axis shows how as solar irradiance increases, the temperature difference between the cooler and the air increases, as the cooler is able to reflect the majority of the sunlight. Adapted by permission from Springer Nature Customer Service Center GmbH: Springer Nature, *Nature*, Passive Radiative Cooling below Ambient Air Temperature under Direct Sunlight, Raman, A. P.; Anoma, M. A.; Zhu, L.; Rephaeli, E.; Fan, S., Copyright 2014 Macmillan Publishers Ltd.

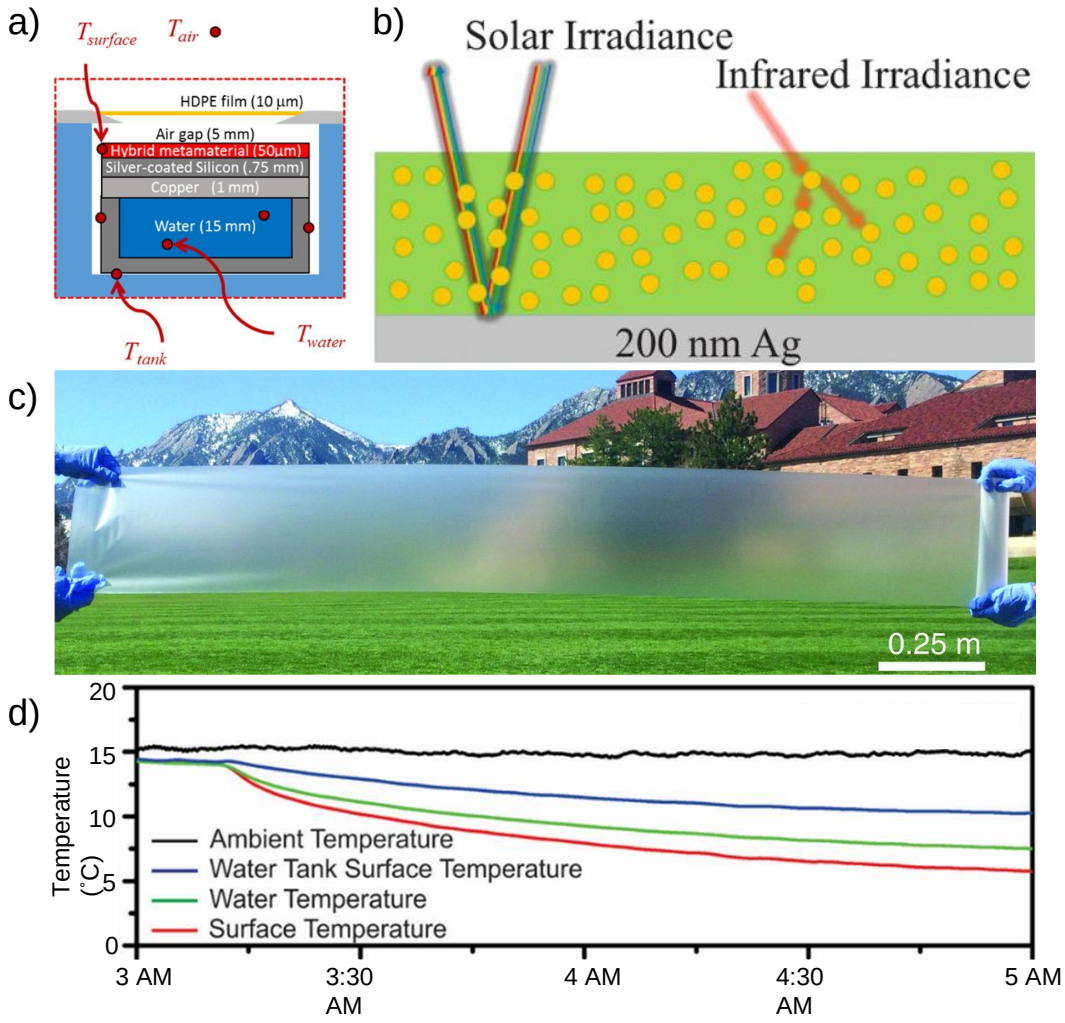

Figure 3.3 Zhai *et. al.* embedded resonant SiO_2 microspheres randomly in a polymethylpentene (TPX) polymer matrix via a roll-to-roll processing method to create a scalable glass-polymer metamaterial that achieves a surface temperature about 9 K below ambient (d), with notably higher cooling power at night.[6] The experimental set-up (a) used to measure radiative cooling power utilized thermocouples to monitor system temperature. The radiated power was equated to the amount of energy pumped into the system to maintain constant water temperature. The metamaterial is illustrated (b) to show its interaction with light and pictured (c). From Zhai, Y.; Ma, Y.; David, S. N.; Zhao, D.; Lou, R.; Tan, G.; Yang, R.; Yin, X. Scalable-Manufactured Randomized Glass-Polymer Hybrid Metamaterial for Daytime Radiative Cooling. Science. 2017, 355, 1062–1066. Reprinted with permission from AAAS.

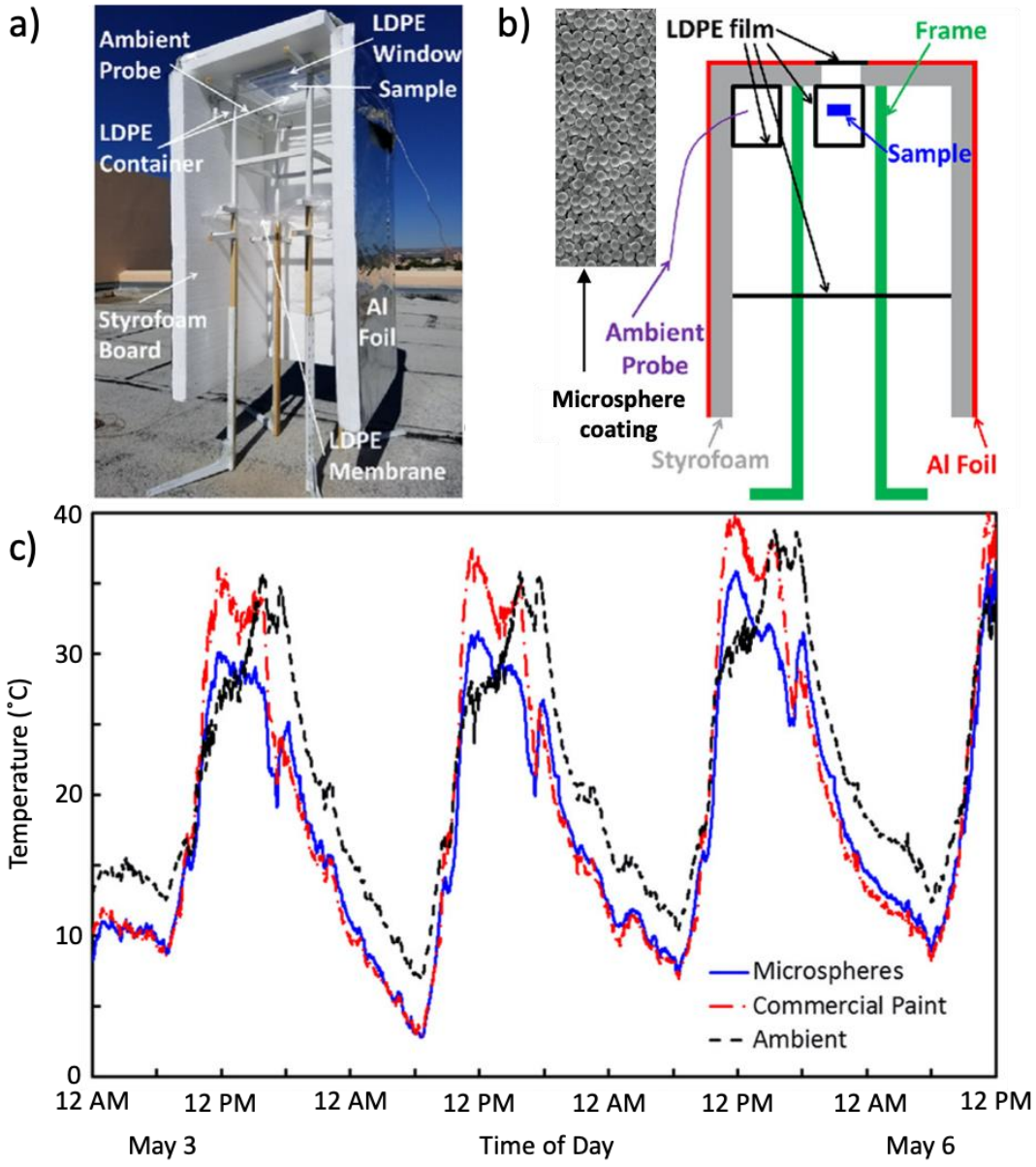

Figure 3.4 Atiganyanun *et. al.* demonstrated that a paint-format SiO_2 microsphere-based coating on a black substrate can reduce the substrate temperature below that of the ambient air by as much as 12°C under sunlight and by 4°C at night while delivering about 100 W/m^2 radiative cooling power.[7] The experimental set-up is pictured (a) and illustrated (b) alongside an SEM image of the SiO_2 microsphere coating. The microspheres were dispersed in a surfactant, which allowed them to be spray-coated onto the substrate. The experiment showed (d) that over the course of 4 days, the microsphere coating outperformed commercial white paint in cooling under direct sunlight. Adapted with permission from Atiganyanun, S.; Plumley, J. B.; Han, S. J.; Hsu, K.; Cytrynbaum, J.; Peng, T. L.; Han, S. M.; Han, S. E. Effective Radiative Cooling by Paint-Format Microsphere-Based Photonic Random Media. *ACS Photonics* **2018,** *5*, 1181-1187. Copyright 2018 American Chemical Society.

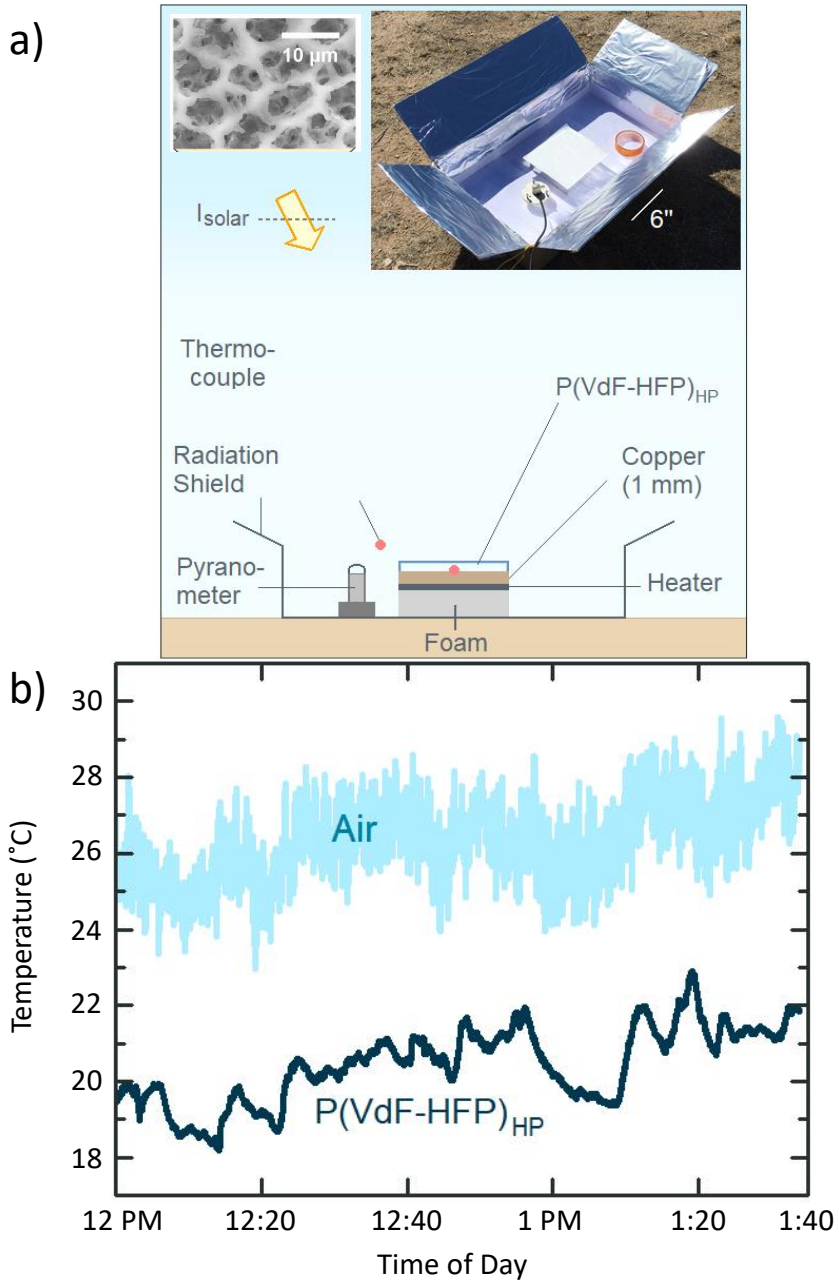

Figure 3.5 Mandal *et. al.* substituted the SiO_2 microspheres used in the experiment featured in Figure 3.3 for air gaps within the polymer matrix and produced a scalable phase-inversion based P(VdF-HFP)$_{HP}$ coating that allows for a sub-ambient temperature drop of 6 K, shown in the plot (b).[8] The experimental set-up is pictured and illustrated (a), along with a micrograph of the porous polymer. From Mandal, J.; Fu, Y.; Overvig, A.; Jia, M.; Sun, K.; Shi, N.; Zhou, H.; Xiao, X.; Yu, N.; Yang, Y. Hierarchically Porous Polymer Coatings for Highly Efficient Passive Daytime Radiative Cooling. Science 2018, 362, 315-319. Reprinted with permission from AAAS.

3.4 Extension to nighttime photovoltaics

For optimal sub-ambient cooling under direct sunlight, a radiative cooler would selectively emit only within the ATW with ε_{LWIR} ~1 and ε ~0 elsewhere. However, for a TR device, the intent of the emission is not to cool it down, but rather to ensure it radiates well in the IR to maximize the radiative power. Furthermore, some radiative coolers, like those highlighted in Figures 3.2 and 3.3, use thin metal layers to reflect incident sunlight for daytime cooling.[5,6] Note that such a requirement is not necessary for nighttime operation of the TR devices we are considering; however, the sun could also be used to heat the TR material if operating during the day, as discussed below, or the solar illumination could be used by another device (e.g. a traditional solar cell), so long as the semiconductor of the TR cell does not absorb the sunlight. The device should emit strongly over thermal wavelengths similar to the behavior of the porous polymer material highlighted in Figure 3.5, which happens naturally for the low-bandgap materials required for power production. For operation under direct sunlight (e.g. to enable 24-hr power production), using the treatment to be outlined in the following chapter we find that R_{solar} as low as 0.5 will allow for the 300 K TR device to produce > 1 W/m^2 power. It must be noted that the optimal bandgap shifts closer to zero as R_{solar} decreases from unity. There is less restriction, however, on the required thermal emissivity due to the several orders of magnitude difference between absorbed and emitted photons. An ε_{IR} of 0.4 will allow for > 1 W/m^2 power production, and the nighttime PV device will produce power, though negligible (< 0.1 W/m^2), with ε_{IR} as low as 0.01. As stated previously, available materials with ε_{IR} > 0.9 are common.

Chapter 4: Fundamental limits

After drawing insight from the existing literature on the methods of radiative cooling covered in the previous chapter, we can now use the formulism described in Section 2.2 to calculate the fundamental limits of a thermoradiative system used to generate power from ambient radiation. This chapter will first discuss the general power limits of such a technology. Next, we discuss the steps needed to adapt these limits to a terrestrial module and calculate the limits of our nighttime photovoltaic cell. Finally, we consider the materials limitations in order to cite practical limits of the technology, given the current understanding of solid-state physics and materials engineering.

4.1 General power limits of a TR PV cell at 300 K

Before discussing the output potential of a terrestrial PV device exposed to the sky, we first calculate the general power limits for a TR system by applying the principle of detailed balance outlined in Section 2.2. We find that an ideal TR cell at 300 K coupled with a 3 K radiating body (deep space) has a maximum power output of 54 W/m^2, and the power output is highest below a bandgap of 0.05 eV (top curve in Figure 4.2). Figure 4.1 shows the maximum power that can be obtained from a TR cell at T_c = 300 K with $0 < E_g \leq 0.25$ eV exposed to a blackbody radiator of temperature 3 K $\leq T_a \leq$ 295 K. We refer to these T_a as effective sky temperatures, which approximate the amount of downwelling (or incident) infrared radiation a terrestrial cell may experience from the atmosphere, space, or another object in the form of a blackbody. While the actual radiation spectrum should be used when available, for simplicity, we

model the total downwelling radiation as a blackbody with an effective sky temperature, T_a (see eq 2.1), where the temperature is chosen to provide the total number of absorbed photons that would be expected from an ambient temperature blackbody with semi-transparent emission windows defined from experimental data at different locations and weather conditions. Note that the optimal bandgap trends away from 0 eV as the effective sky temperature increases from 3 K. As effective sky temperature increases, so does the peak of its emission spectrum, and thus the average number of incident photons on the cell increases. With low bandgap semiconductors, these photons will be increasingly absorbed by the cell, which will decrease the cell's power output, as its own emission does not increase at the same rate. Increasing the bandgap of the semiconductor with the effective sky temperature thus limits the absorption of these increasingly energetic incident photons, and so the max power point is found at an increasingly higher bandgap. For a TR PV cell at 300 K to produce a useful amount of power, the material bandgap needs to be less than 0.1 eV.

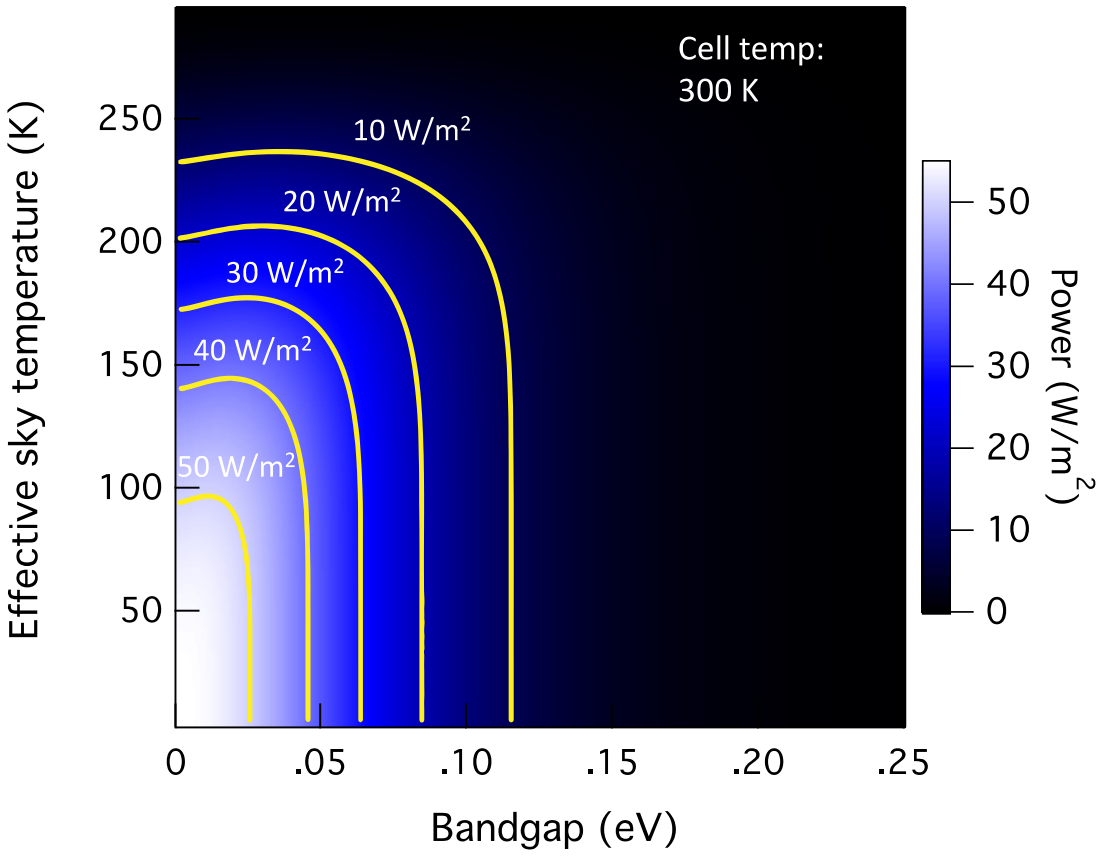

Figure 4.1 Maximum power output of a thermoradiative cell, held at 300 K, whose semiconductor bandgap ranges from 0 to 0.25 eV for effective sky temperatures 3 to 295 K. The optimal bandgap increases as effective sky temperature increases, showing broadening contour lines. Tristan Deppe and Jeremy N. Munday. Nighttime Photovoltaic Cells: Electrical Power Generation by Optically Coupling with Deep Space. *ACS Photonics* 2020, *7*, 1, 1-9.

4.2 Terrestrial limits

While coupling directly with deep space at 3 K is optimal for power conversion, the 54 W/m^2 target calculated in the previous section is only obtainable for an extra-terrestrial device held at 300 K. Due to the emission spectrum of the atmosphere, for a terrestrial device to directly access the darkness of space, we could restrict its emissivity to only the ATW using a selective emitter; however, this results in a

significantly lower maximum power output of 11.8 W/m^2 (for a material with E_g = 0.095 eV), assuming zero emission from the sky within the window, which is however unlikely. To determine the maximum achievable power for a terrestrial cell exposed to the sky, we return to the concept of radiative cooling and a more precise analysis of atmospheric emission.

4.2.1 Sky emission

To accurately model the terrestrial TR device, we must now consider the amount of thermal radiation from the sky incident on the earth's surface. Outside of the atmospheric transparency window, the sky's emission resembles that of a blackbody at the ambient air temperature. Within the window, though the upper levels of the atmosphere are transparent to LWIR, these wavelengths are absorbed and emitted by water molecules present in varying concentrations throughout the troposphere, the lowest level of the atmosphere, in the form of humidity, fog, and, most notably, cloud cover. Thermal emission from clouds depends on the optical depth and altitude; optically thick clouds have high emission and optically thin clouds, typically at higher altitudes and colder temperatures, have lower emission.[21] Therefore the earth's cooling power, which is the difference between the outgoing radiation and the downwelling power, and the performance of a terrestrial TR cell rely on local weather conditions; optimal conditions would be clear skies and low humidity.

4.2.2 Terrestrial effective sky temperatures

At 300 K ambient temperatures, broadband cooling powers of 160 W/m^2 and >120 W/m^2 have been estimated[22,23] and measured,[6] respectively. In general, without

detailed sky emission measurements, we can use the cooling powers to extract an effective sky temperature that simulates real sky conditions. To do this, we first define the cooling power as the difference in power emitted from a blackbody at 300 K and one at T_a and then use Planck's law to solve for T_a. To calculate extractable electrical power, we follow the principles of detailed balance and use eq 2.3, this time with an ideal broadband cell emissivity of $\varepsilon = 1$ for wavelengths greater than 3 μm and $\varepsilon = 0$ elsewhere, simulating a perfect solar reflector (or transmitter) and IR emitter. We find that under the real sky conditions measured in Colorado, i.e. a broadband cooling power of 130 W/m^2 at 300 K ambient,[6] which corresponds to an effective sky temperature of 276 K, an ideal broadband TR cell held at the ambient 300 K and pointed at the sky has a power output >2 W/m^2. This number increases to 3.2 W/m^2 if we use the predicted maximum net cooling rate of 160 W/m^2 for 300 K ambient, corresponding to an effective sky temperature of 270 K, achievable under optimal weather conditions. Figure 4.2 highlights the maximum extractable power for broadband coupling with selected effective sky temperatures that simulate different conditions: the ideal deep space (no atmosphere) at 3 K, clear skies and low humidity, i.e. optimal conditions, at 270 K, and a humid suburban sky at 290 K. This last effective sky temperature (290 K) was chosen by using a lower cooling power of 60 W/m^2, which is consistent with inserting overcast weather conditions into the modified Swinbank model for downwelling IR and computing an effective sky temperature according to Stefan's law (see Appendix A).[24,25]

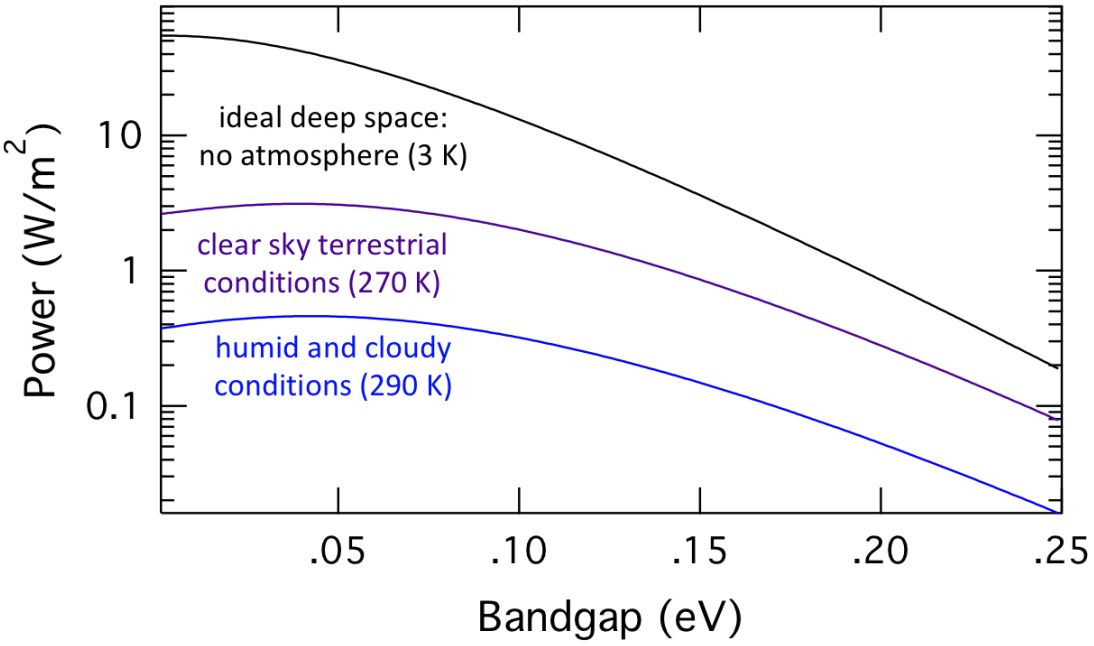

Figure 4.2 Maximum power density vs bandgap energy for a 300 K terrestrial cell and three selected sky conditions, modeled with effective sky temperatures. The ideal case is a cell directly accessing the darkness of space at 3 K. 270 K simulates clear terrestrial conditions, extrapolated from maximum radiative cooling estimates.[22,23] 290 K corresponds to humid and overcast conditions. Tristan Deppe and Jeremy N. Munday. Nighttime Photovoltaic Cells: Electrical Power Generation by Optically Coupling with Deep Space. *ACS Photonics* 2020, *7***,** 1, 1-9.

4.2.3 Selective emission power limits

To more accurately estimate power production, further detailed sky emission information is required. Terrestrial measurements of downwelling atmospheric LWIR are not common, however 24-hr averages of approximately 35 W/m^2 in the winter and 75 W/m^2 in the summer, with respective surface temperatures of 285 K and 300 K, between 8 and 13 μm have been reported at the ARM Climate Research Facility in Lamont, OK.[26] Multiplying eq 2.1 by photon energy and this time integrating over the transparency window, these power measurements correspond to blackbodies of T_a =

223 K and 262 K, which we can use as T_a in eq 2.3 to simulate the incident radiation on the device. To calculate extractable power, we again apply the principles of detailed balance, and, restricting cell emissivity such that $\varepsilon_{LWIR} = 1$ and $\varepsilon = 0$ outside the ATW, we calculate an extractable power in Lamont, OK of 3.2 and 1.6 W/m^2 in the winter and summer, respectively. In these cases, the net cooling power within the window is approximately 80 W/m^2. If the estimated max cooling power of 140 W/m^2 within the ATW is assumed,[23] a 300 K cell could potentially extract up to 10 W/m^2 by accessing the atmospheric transparency window alone. In this case, when we restrict emission to the window using a selective emitter, the maximum power is achieved using a material of bandgap $E_g = 0.095$ eV.

4.2.4 Additional notes

We note that, under any terrestrial configuration, the TR device is not coupling directly with deep space, but rather with the atmosphere. Because sky emission and the effective sky temperature fluctuate significantly with weather conditions and the optimal bandgap increases with effective sky temperature, optimization of a TR cell will depend on the environmental conditions (e.g. cloud cover, humidity, ground temperature, etc.) under which the cell will be operating. Much like a conventional solar cell, the power conversion ability of a TR device is dramatically reduced by cloud cover.

4.3 Materials limits

Up to this point in the discussion, we have considered only the radiative generation-recombination processes for creating or removing electron-hole pairs that are not collected through current extraction. We complete the analysis by discussing the effects of non-radiative generation and recombination.

4.3.1 Non-radiative processes

Auger recombination (and the inverse process of impact ionization) is considered the dominant non-radiative process in low bandgap semiconductors, especially near room temperature.[27] To account for this process, eq 2.3 is modified to include a non-radiative generation term, $\dot{N}_{NR}$, such that the total power output is

$$P = JV = qV\left[\dot{N}(T_a, 0) - \dot{N}(T_c, qV) + \dot{N}_{NR}\right]. \tag{4.1}$$

While $\dot{N}_{NR}$ would be a function of voltage for an actual *p-n* device, we have suppressed this dependance to focus on the fraction of non-radiatively generated carriers by defining the non-radiative generation ratio

$$\eta \equiv \frac{\dot{N}_{NR}}{\dot{N}(T_a,0)+\dot{N}_{NR}}, \tag{4.2}$$

such that the total power output becomes

$$P = qV\left[\left(\frac{1}{1-\eta}\right)\dot{N}(T_a, 0) - \dot{N}(T_c, qV)\right]. \tag{4.3}$$

Figure 4.3 shows how the extractable power decreases as non-radiative generation/recombination rates increase for a cell operating under realistic weather conditions, i.e. effective sky temperature of 270 K.

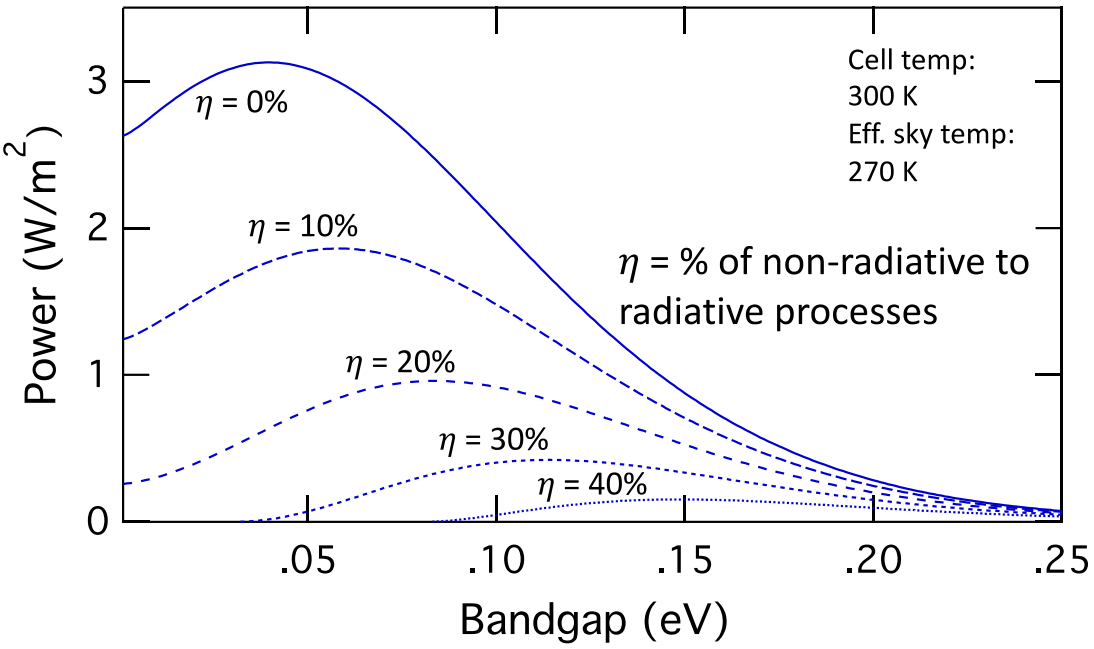

Figure 4.3 Power output for different percentages of non-radiative generation, η, for a thermoradiative device operating at 300 K exposed to a sky with effective temperature of 270 K, simulating clear sky conditions.[22,23] Tristan Deppe and Jeremy N. Munday. Nighttime Photovoltaic Cells: Electrical Power Generation by Optically Coupling with Deep Space. *ACS Photonics* 2020, *7***,** 1, 1-9.

4.3.2 Practical limits

Next we consider what levels of non-radiative generation/recombination can be expected in real devices. Tennant showed that reverse-bias leakage currents in experimental IR photodetectors follow an exponential trend, called the "Rule 07," that increases with decreasing bandgap and increasing device temperature.[27,28] Comparing this exponential fit to the calculated radiative current densities of our TR device, it appears that non-radiative processes would outweigh the radiative ones by a factor of up to 10^4 in the optimal bandgap regime of ~0.04 eV, and up to 10^3 for E_g ~0.1 eV in the best case scenario (Figure 4.4).

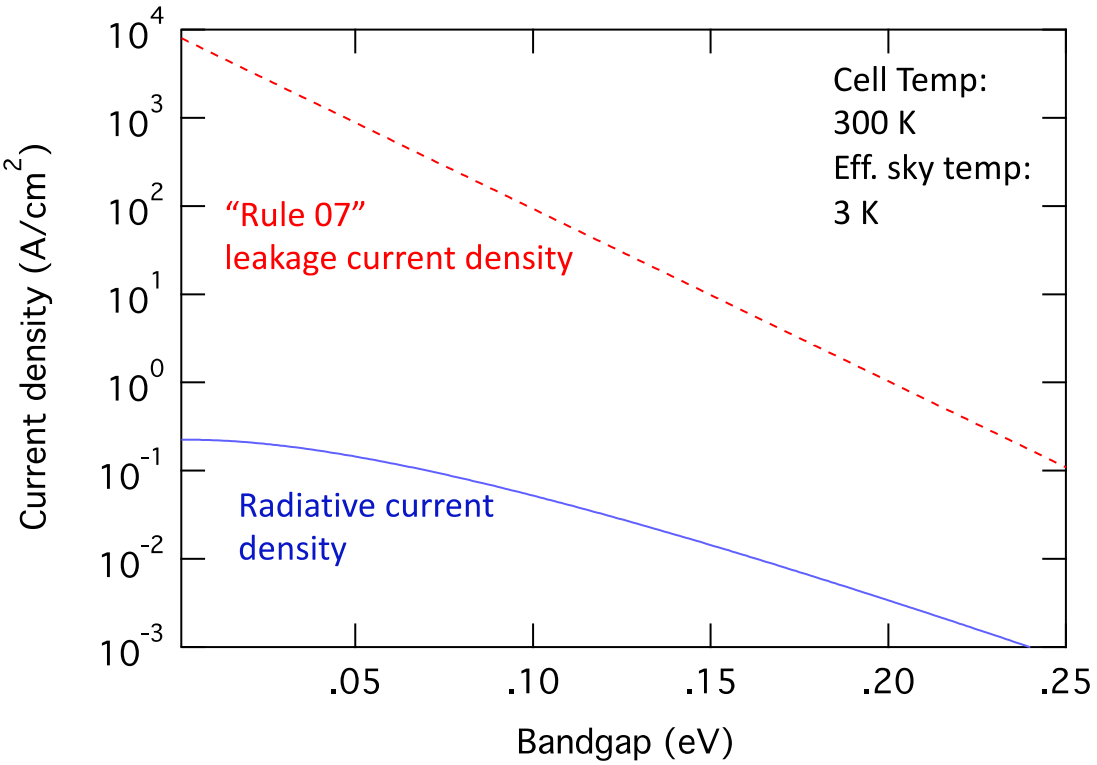

Figure 4.4 Compares the predicted reverse-bias leakage current densities for low bandgap devices, following the trend for experimental IR photodetectors, known as "Rule 07,"[27,28] with the calculated radiative current density for an ideal TR device of the same bandgaps energies.

However, the previously mentioned experiment performed by Santhanam and Fan, showed an extractable power that corresponds to a non-radiative generation percentage of 3%, in accordance with the above treatment (eq 4.2), compared to η ~99%, as predicted with Rule 07. This result suggests that although non-radiative processes are present in these materials, they may not significantly inhibit the development of TR devices. Additionally, regarding device improvement, significant Auger suppression has been demonstated in low-gap semiconductors under strong reverse bias.[29] However our operating voltage is around 1 k_BT (see Appendix B), so new materials developments, such as quantum wells, which predict a suppression of

the Auger mechanism by two orders of magnitude,[30] may be useful in order to keep the non-radiative generation rate low. Compared to bulk materials, the room temperature Auger recombination coefficients of type-II InAs-$Ga_{1-x}In_xSb$-InAs-AlSb quantum well lasers (E_g ~0.28 eV) and InAs/GaSb superlattice photoconductors (E_g ~0.1 eV) have been reduced by a factor of four[31] and eight,[32] respectively, through appropriate engineering. These experimental results lead to the conclusion that a well-designed TR device, built purely with existing materials and engineering methods, such as the InAs/GaSb superlattice, could conceivably produce 1.5 W/m^2 in the broadband configuration or potentially up to 8.4 W/m^2 with selective emission under the night sky.

Chapter 5: Scalability – Materials and Integration

The underlying functionality of the TR cell relies on maintaining the temperature difference between the cell and the sky. As with any radiating body facing a colder environment, the cell loses energy as it emits, so in order to maintain the cell temperature, it must be in thermal contact with the earth at a fixed temperature (e.g. at 300 K). Further, the top surface of the cell must be optically coupled to the sky. These criteria thus suggest a module that: (i) is thermally conducting on the bottom surface, which can include a back-reflector to direct the cell's radiation towards the sky, (ii) is encapsulated to protect the cell from the environment and restrict conductive and convective heat loss, and (iii) includes an infrared window on the front to allow radiative heat transfer to the sky.

5.1 Materials

For the active material, there are several possible low bandgap semiconductors that could serve as starting points for investigation. InSb can reach a bandgap below 0.1 eV,[33] which can be useful in proof of principle devices. However, for optimal power, even lower bandgaps are needed. $Hg_{1-x}Cd_xTe$, a heavily characterized material used in the infrared sensing industry, can be bandgap engineered into the realm needed for a high-power-producing TR cell with a Cd composition of around $x = 0.1$.[34] Newer materials that can have even lower bandgaps, such as graphene-hBN (hexagonal Boron-Nitride) heterostructures, could also prove useful in a TR device. Although difficult to fabricate, it has been shown that alternately stacking sheets of graphene with hBN can open a bandgap of 0.04 eV in the graphene layer,[35-37] which would be an

excellent bandgap for a nighttime PV cell. However, any chosen material may likely need additional engineering in order to suppress non-radiative processes.

For the top surface material that provides radiative access to the sky and reflects solar radiation, it has been discussed previously that many materials, such as those detailed in Figures 3.3, 3.4, and 3.5 or the commercially available thermoplastic and polymer materials (see Reference 17 for a complete list of industrial-grade cooling materials on the market) offer the necessary emission and reflection characteristics as well as the scalability required for large-scale production.

5.2 Integration

If the cell can be constructed to operate at higher temperatures, it could generate even more power, as shown in Figure 5.1. Notably, if sunlight is used to heat the cell up to 330 K, the maximum power increases to 13.3 W/m^2 for a 270 K effective sky temperature. If connected to an external heat source (or concentrated solar) and operating at T_c = 471 K, the maximum power reaches 200 W/m^2. Additionally, these higher operating temperatures allow for greater power generation at larger bandgaps. At an operating temperature of 443 K, a material with a bandgap of 0.1 eV could produce 100 W/m^2. At this temperature InSb, with E_g = 0.17, could directly produce 40 W/m^2 without additional bandgap engineering. Possible configurations for such devices are sketched in Figure 5.2. Further, instead of using the sun as a heat source, one can also envision attaching these devices to industrial exhaust systems, consistently at high temperatures, and pointing them towards the sky in order to extract additional power from the wasted heat of the industrial process.

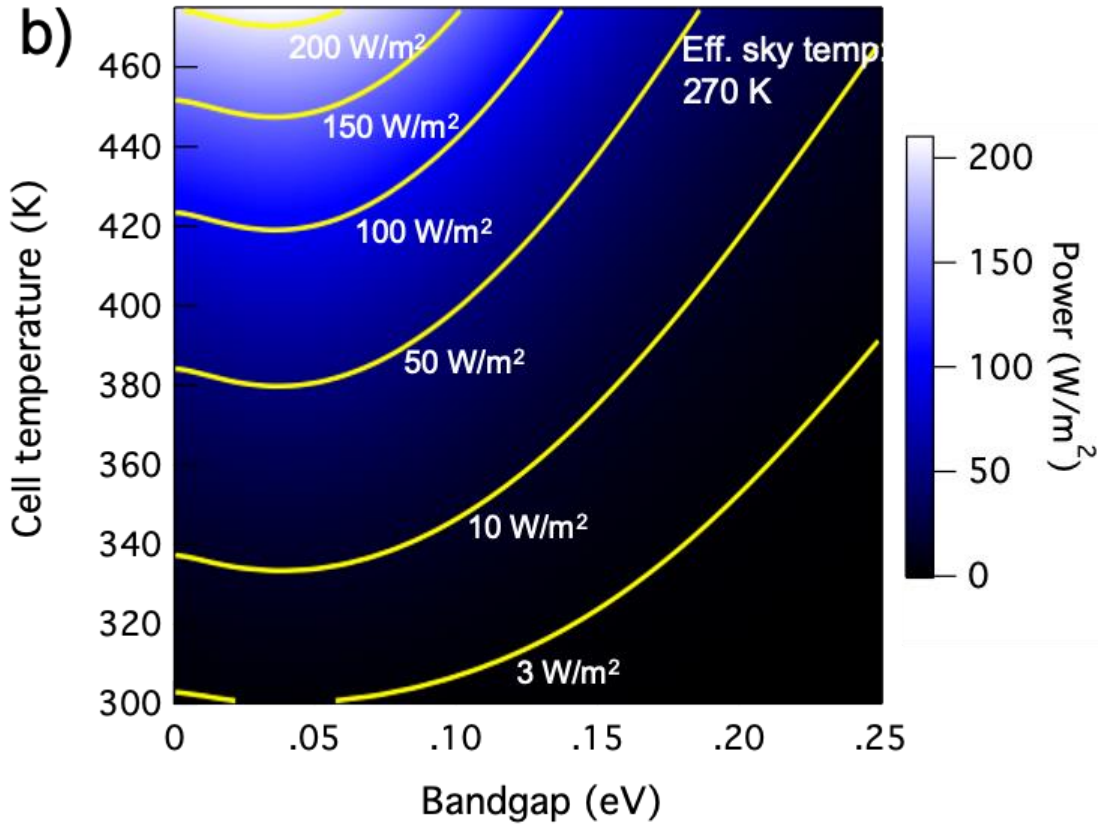

Figure 5.1 Maximum power output of a thermoradiative cell at a range of temperatures, coupled with the sky at an effective temperature of 270 K, simulating clear sky conditions.[22,23] Contour lines show how bandgap relates to power output as cell temperature increases. Tristan Deppe and Jeremy N. Munday. Nighttime Photovoltaic Cells: Electrical Power Generation by Optically Coupling with Deep Space. *ACS Photonics* 2020, *7***,** 1, 1-9.

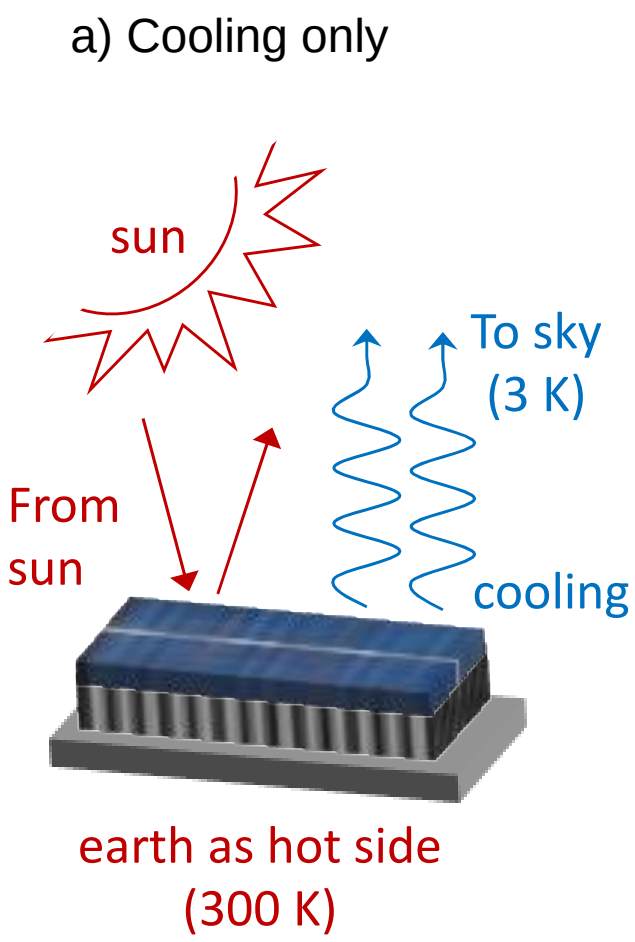

Figure 5.2a Conceptual design for a thermoradiative cell configuration. The basic design, assumed throughout the calculations in this paper, includes a "hot side" that is in thermal contact with earth while the top of the cell can radiate thermal power to deep space. Tristan Deppe and Jeremy N. Munday. Nighttime Photovoltaic Cells: Electrical Power Generation by Optically Coupling with Deep Space. *ACS Photonics* 2020, *7*, 1, 1-9.

b) Cooling and heating

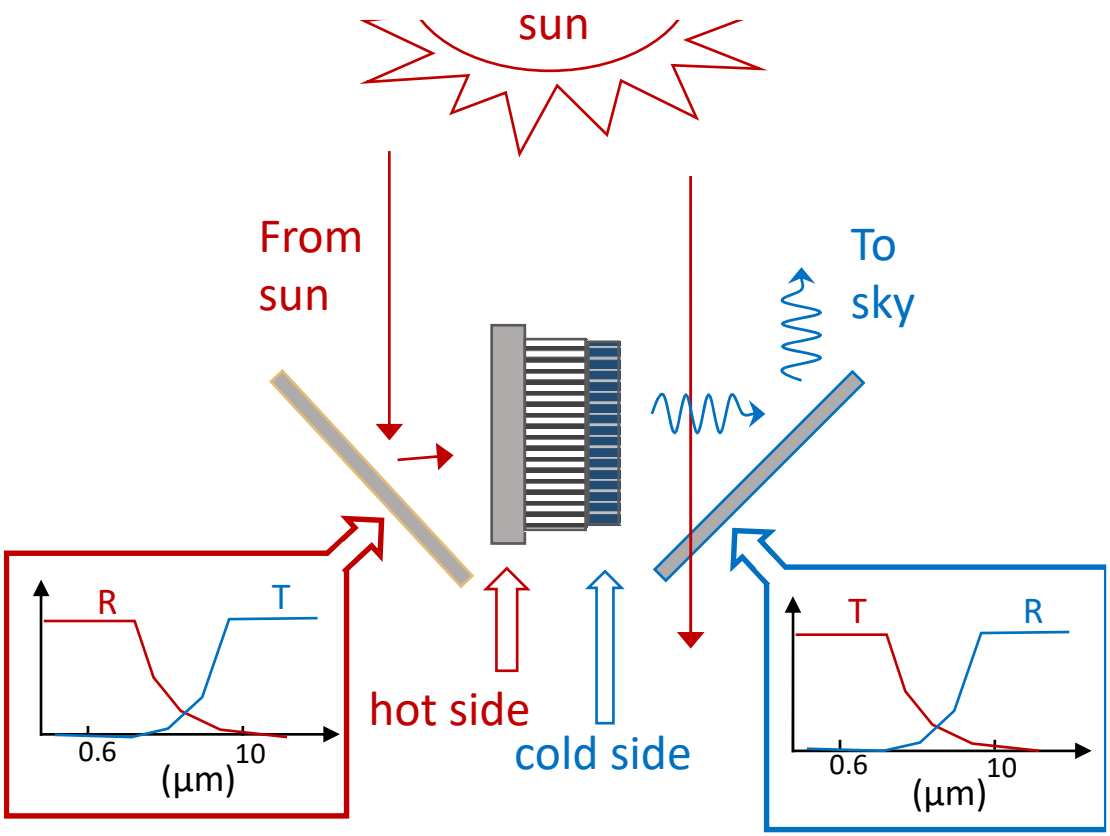

Figure 5.2b Conceptual design for a thermoradiative cell configuration. Rotating the cell and using spectrally selective optical reflectors, we can heat up the "hot side" of the cell during the day to enhance power generation. A mirror that reflects the sun's irradiance towards the cell heats one side while a corresponding mirror transmits the solar irradiance and reflects the thermal emission from the cell towards deep space. In this configuration, a selective solar absorber, a material with high solar absorbance and low thermal emittance,[38] could be used as the cell's hot side. Tristan Deppe and Jeremy N. Munday. Nighttime Photovoltaic Cells: Electrical Power Generation by Optically Coupling with Deep Space. *ACS Photonics* 2020, *7***,** 1, 1-9.

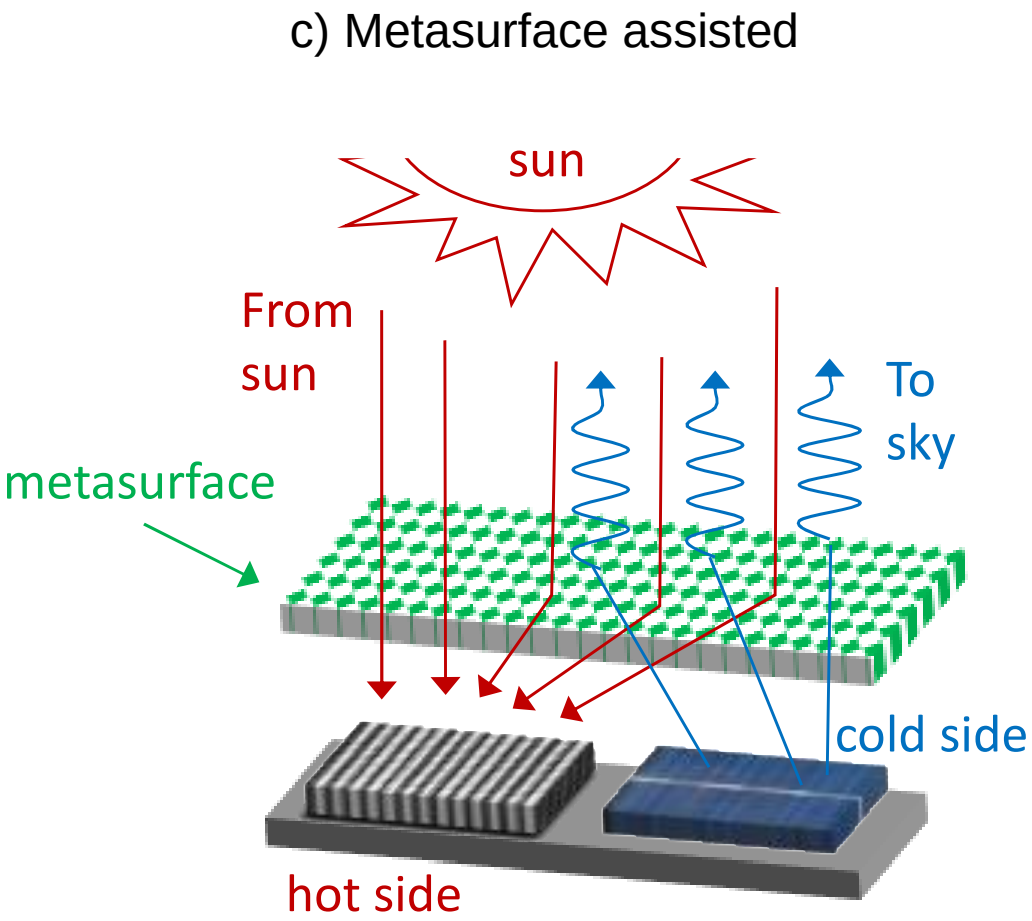

Figure 5.2c Conceptual design for a thermoradiative cell configuration. (c) This effect could also be performed more compactly using metamaterials. A metamaterial can be engineered to direct solar irradiance passing through it towards one side of the device while directing thermal radiation from the cell back towards deep space, allowing for a planar cell design where one half is for heating and the other is for thermal emission. Tristan Deppe and Jeremy N. Munday. Nighttime Photovoltaic Cells: Electrical Power Generation by Optically Coupling with Deep Space. *ACS Photonics* 2020, *7***,** 1, 1-9.

Alternatively, instead of competing with traditional PV for power production, a nighttime PV module could be coupled with existing PV in order to maximize the 24-hr power cycle. In open, arid environments, where solar farms are already common, the effective sky temperature is low enough to provide for near-ideal TR power production. If a retractable nighttime PV unit were rolled out on top of the standard solar modules after sunset, a solar farm could produce an additional 12% more electricity. More power can be generated if a heterojunction cell can be engineered, allowing both the conventional PV cell, on top, and the TR PV cell, on bottom, to work in tandem during the day. The higher bandgap material will absorb the sunlight but will be transparent to the lower energy thermal photons, which will allow the TR PV cell on bottom to generate power night and day, adding 24% more electricity to the daily power cycle.

Chapter 6: Impact and future work

The largest challenge facing the implementation of this technology is the development of stable low-bandgap materials, with *Eg* around or below 0.1 eV. As mentioned in Section 4.3.1, non-radiative processes dominate over radiative processes for room-temperature materials with bandgap in the range necessary for power production, so significant materials engineering will likely be needed to approach the theoretical limits. However, existing materials should prove useful for proof of principle experiments. Comparing current output with the expected leakage current (see "Rule 07") can shed more light on the effect of non-radiative processes on thermoradiative photovoltaic power production.

Additionally, for effective power generation, radiative emission must be the major source of heat loss for the top surface. This effect can be achieved easily by running the experiment under vacuum to restrict convective and conductive heat loss. An IR-transparent window on the top of the chamber can then be used to enable optical coupling with the sky.

In conclusion, as the global push towards carbon neutrality continues, the sun is not the only sky-facing option for power generation. Thermoradiative photovoltaic devices offer the possibility of nighttime power generation by optically coupling with the cold of deep space (or the cool atmosphere). Such devices need strong absorption and emission at thermal wavelengths and clear and dry conditions to facilitate optical access to the night sky and high rates of cooling. Because radiative cooling is centered on the atmospheric transparency window between 8 and 13 μm, radiative emission should be restricted to this window as well in order to optimize power generation and

reach the 10 W/m^2 target for 300 K ambient temperatures. This can be achieved by ensuring that the emitter surface of the device has emissivity approaching unity within the ATW and approximately zero outside. In this configuration, an energy gap of 0.095 eV is ideal for the active material, as this energy aligns with the lower edge of the atmospheric transparency window of 13 μm. This helps restrict emission to the ATW, allows for higher operating voltages, and is high enough to alleviate some of the concern about non-radiative generation, which hurts low-bandgap device performance. For optimal operation during the day, in addition to the previous characteristics, the active layer of the device should also have reflectivity that approaches unity for wavelengths <3 μm. Night or day, if the cell can be heated to a higher temperature, either from allowing the device to heat up under the sun or absorb waste heat from industrial and residential sources, the device has the possibility to generate even more power. This occurs when cell temperature increases but sky temperature remains constant, and the net power flow from the cell to the sky increases.

As shown throughout this thesis, deep space offers an intriguing low-temperature thermal sink that has the potential to help provide electrical power at night and day through the clever use of photonics, optics, and materials science.

Appendix A: Model for Effective Sky Temperature

The modified Swinbank formula estimates downwelling atmospheric radiation as[24]

$$P_{rad} = (1 + KC^2)\ 8.78\ x\ 10^{-13}\ {T_{air}}^{5.852} RH^{0.07195} \quad \text{(A1)}$$

where K is a measure of cloud height, ranging from 0.06 for very high to 0.34 for very low, C is the fraction of sky covered by clouds, T_{air} is the ambient air temperature, and RH is the relative humidity (as a percentage). Inserting the conditions for clear skies (C = 0) and low, desert-like humidity of 5%, the model estimates a downwelling radiation for ambient air temperature of 300 K to be 309 W/m^2. Overcast and humid conditions (K = .2, C = 0.7, RH = 55) result in a downwelling radiance of 406 W/m^2. We can insert these powers into the Planck formula for blackbody radiation,

$$\dot{E}(T) = \frac{2\pi}{h^3 c^2} \int_0^\infty \frac{E^3}{e^{\frac{E}{k_B T}} - 1} dE, \quad \text{(A2)}$$

and solve for T to find the corresponding effective sky temperatures. We calculate 271 K for the optimal clear sky conditions, which corresponds well to the effective sky temperature of 270 K extracted from radiative cooling estimates which we use for the calculations of the power limits throughout the paper. The overcast and humid conditions correspond to 290 K, which we use to calculate the bottom curve in Figure 4.2 which shows the power output of a cell operating in humid and overcast conditions.

Appendix B: Additional Figures

The following figures provide a complete analysis of TR cell function, analogous to those provided for conventional solar cells. Figure B1 shows power alongside efficiency, which was ignored in the greater text. Figure B2 shows how operating current and operating voltage change with bandgap, and Figure B3 provides an IV curve for an optimized device. All calculations were performed using cell temperature of 300 K and an effective sky temperature of 270 K.

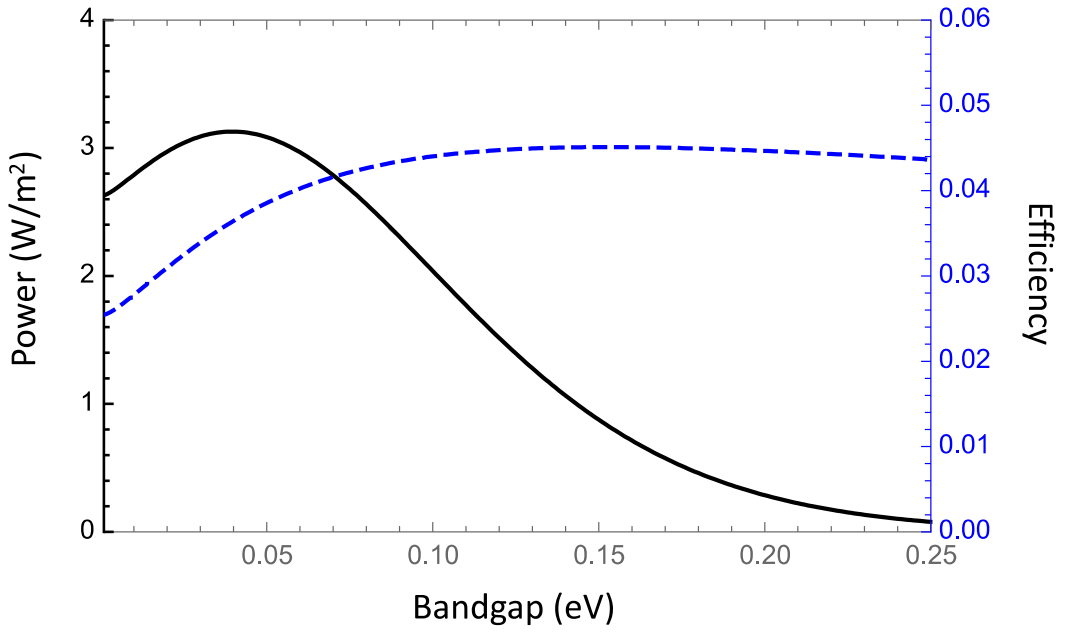

Figure B1 A plot of the maximum extractable power and efficiency vs bandgap (eV) of a terrestrial cell at 300 K facing the sky with effective sky temperature of 270 K, corresponding to clear skies and low humidity.

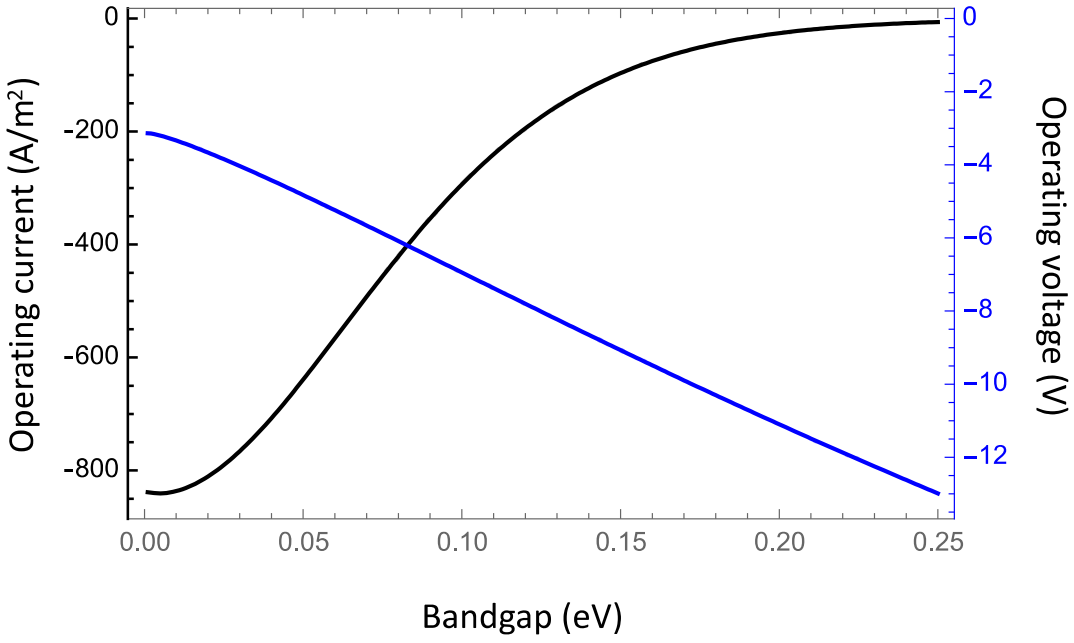

Figure B2 The operating current and operating voltage as a function of material bandgap for a 300 K terrestrial cell facing the sky with effective sky temperature 270 K.

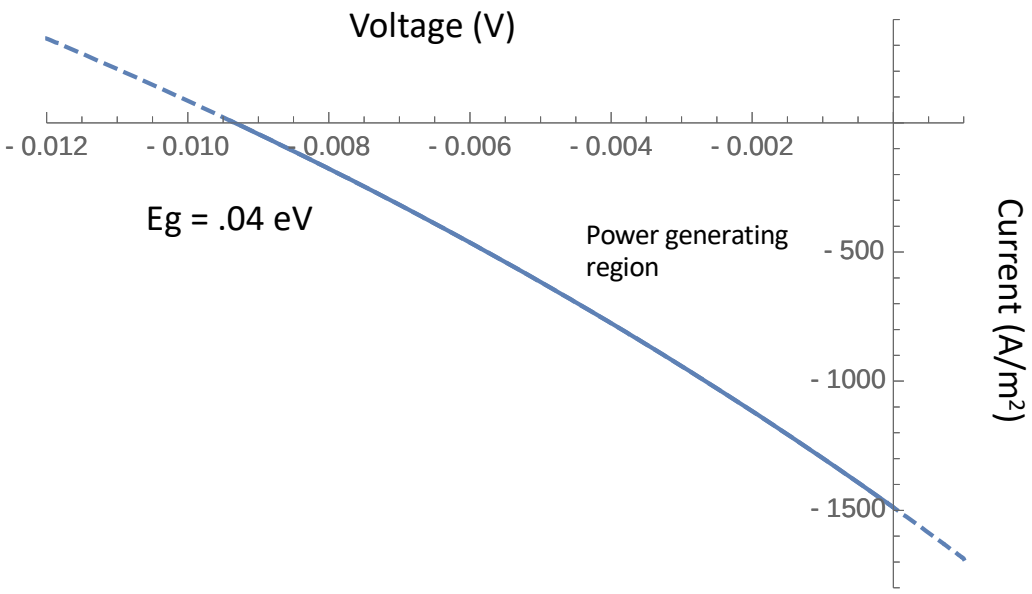

Figure B3 IV curve for a 300 K cell, with material bandgap 0.04 eV, facing a 270 K sky. 0.04 eV is the optimal bandgap for these conditions. The power generating region occurs between -0.0094 V and 0 V.

Bibliography

1. Shockley, W.; Queisser, H. J. Detailed Balance Limit of Efficiency of P-n Junction Solar Cells. *J. Appl. Phys.* **1961,** *32*, 510–519.
2. Strandberg, R. Theoretical Efficiency Limits for Thermoradiative Energy Conversion. *J. Appl. Phys.* **2015,** *117*, 055105.
3. National Renewable Energy Laboratory. U.S. State Solar Resource Maps. https://www.nrel.gov/gis/solar.html (accessed Jun 27, 2019).
4. Bahadori, M. N. Passive Cooling Systems in Iranian Architecture. *Sci. Am.* **1978,** *238*, 144–154.
5. Raman, A. P.; Anoma, M. A.; Zhu, L.; Rephaeli, E.; Fan, S. Passive Radiative Cooling below Ambient Air Temperature under Direct Sunlight. *Nature* **2014,** *515*, 540–544.
6. Zhai, Y.; Ma, Y.; David, S. N.; Zhao, D.; Lou, R.; Tan, G.; Yang, R.; Yin, X. Scalable-Manufactured Randomized Glass-Polymer Hybrid Metamaterial for Daytime Radiative Cooling. *Science.* **2017,** *355*, 1062–1066.
7. Atiganyanun, S.; Plumley, J. B.; Han, S. J.; Hsu, K.; Cytrynbaum, J.; Peng, T. L.; Han, S. M.; Han, S. E. Effective Radiative Cooling by Paint-Format Microsphere-Based Photonic Random Media. *ACS Photonics* **2018,** *5*, 1181-1187.
8. Mandal, J.; Fu, Y.; Overvig, A.; Jia, M.; Sun, K.; Shi, N.; Zhou, H.; Xiao, X.; Yu, N.; Yang, Y. Hierarchically Porous Polymer Coatings for Highly Efficient Passive Daytime Radiative Cooling. *Science* **2018,** *362*, 315-319.

9. Zhu, L.; Raman, A. P.; Fan, S. Radiative Cooling of Solar Absorbers Using a Visibly Transparent Photonic Crystal Thermal Blackbody. *Proc. Natl. Acad. Sci.* **2015,** *112*, 12282-12287.
10. Safi, T. S.; Munday, J. N. Improving Photovoltaic Performance through Radiative Cooling in Both Terrestrial and Extraterrestrial Environments. *Opt. Express* **2015,** *23*, A1120-A1128.
11. Lin, C.; Wang, B.; Teo, K. H.; Zhang, Z. Performance Comparison Between Photovoltaic and Thermoradiative Devices. *J. Appl. Phys.* **2017,** *122*, 243103
12. Zhang, X.; Peng, W.; Lin, J.; Chen, X.; Chen, J. Parametric Design Criteria of an Updated Thermoradiative Cell Operating at Optimal States. *J. Appl. Phys.* **2017,** *122*, 174505.
13. Hsu, W. C.; Tong, J. K.; Liao, B.; Huang, Y.; Boriskina, S. V.; Chen, G. Entropic and Near-Field Improvements of Thermoradiative Cells. *Sci. Rep.* **2016,** *6*, 34837.
14. Santhanam, P.; Fan, S. Thermal-to-Electrical Energy Conversion by Diodes under Negative Illumination. *Phys. Rev. B* **2016,** *93*, 161410.
15. Würfel, P. Thermodynamic Limitations to Solar Energy Conversion. *Physica E: Low-Dimensional Systems and Nanostructures.* **2002,** *14*, 18-26.
16. Munday, J. N. Tackling Climate Change through Radiative Cooling. *Joule* (in press), DOI:https://doi.org/10.1016/j.joule.2019.07.010
17. Cool Roof Rating Council. Rated Products Directory. https://coolroofs.org/directory (accessed Jul 12, 2019).

18. Yu, N.; Mandal, J.; Overvig, A; Shi, Norman N. Systems and Methods for Radiative Cooling and Heating. WO 2016205717 A1, December 22, 2016.
19. Grenier, P. Réfrigération Radiative. Effet de Serre Inverse. *Rev. Phys. Appliquée.* **1979,** *14*, 87-90.
20. Gentle, A. R.; Smith, G. B. Radiative Heat Pumping from the Earth Using Surface Phonon Resonant Nanoparticles. *Nano Lett.* **2010,** *10*, 373-379.
21. Nugent, P. W.; Shaw, J. a.; Piazzolla, S. Infrared Cloud Imager Development for Atmospheric Optical Communication Characterization, and Measurements at the JPL Table Mountain Facility. *IPN Prog. Rep.* **2013,** *42*, 1-31.
22. Sun, X.; Sun, Y.; Zhou, Z.; Alam, M. A.; Bermel, P. Radiative Sky Cooling: Fundamental physics, materials, structures, and applications. *Nanophotonics.* **2017,** *6*, 997-1015.
23. Zhao, D.; Aili, A.; Zhai, Y.; Xu, S.; Tan, G.; Yin, X.; Yang, R. Radiative sky cooling: Fundamental principles, materials, and applications. *Appl. Phys. Rev.* **2019,** *6*, 021306.
24. Goforth, M. A.; Gilchrist, G.W.; Sirianni, J. D. Cloud Effects on Thermal Downwelling Sky Radiance. *Thermosense XXIV.* **2002,** *4710,* 203-213.
25. Pandey, D. K.; Lee, R. B.; Paden, J. Effects of Atmospheric Emissivity on Clear Sky Temperatures. *Atmos. Environ.* **1995,** *29*, 2201-2204.
26. Byrnes, S. J.; Blanchard, R.; Capasso, F. Harvesting Renewable Energy from Earth's Mid Infrared Emissions. *Proc. Natl. Acad. Sci.* **2014,** *111*, 3927-3932.
27. Tennant, W. E. "Rule 07"' Revisited: Still a Good Heuristic Predictor of p/n HgCdTe Photodiode Performance? *J. Electron. Mater.* **2010,** *39*, 1030-1035.

28. Teherani, J. T.; Agarwal, S.; Chern, W.; Solomon, P. M.; Yablonovitch, E.; Antoniadis, D. A. Auger Generation as an Intrinsic Limit to Tunneling Field-Effect Transistor Performance. *J. Appl. Phys.* **2016,** *120*, 084507.
29. Emelie, P. Y.; Phillips, J.; Velicu, S.; Wijewarnasuriya, P. S. Parameter Extraction of HgCdTe Infrared Photodiodes Exhibiting Auger Suppression. *J. Phys. D: Appl. Phys.* **2009,** *42*, 8.
30. Chiu, L. C.; Amnon Yariv, A. Y. Auger Recombination in Quantum-Well InGaAsP Heterostructure Lasers. *IEEE J. Quantum Electron.* **1982,** *18*, 1406-1409.
31. Felix, C. L.; Meyer, J. R.; Vurgaftman, I.; Lin, C. H.; Murry, S. J.; Zhang, D.; Pei, S. S. High-Temperature 4.5-Mm Type-II Quantum-Well Laser with Auger Suppression. *IEEE Photonics Technol. Lett.* **1997,** *9*, 734-736.
32. Mohseni, H.; Litvinov, V.; Razeghi, M. Interface-Induced Suppression of the Auger Recombination in Type-II InAs/GaSb Superlattices. *Phys. Rev. B: Condens. Matter Mater. Phys.* **1998,** *58*, 378-380.
33. Jin, Y. J.; Tang, X. H.; Ke, C.; Yu, S. Y.; Zhang, D. H. Bandgap Engineering of InSb by N Incorporation by Metal-Organic Chemical Vapor Deposition. *J. Alloys Compd.* **2018,** *756*, 134-138.
34. Norton, P. HgCdTe Infrared Detectors. *Opto-Electron. Rev.* **2002,** *10,* 159-174.
35. Cassabois, G.; Valvin, P.; Gil, B. Hexagonal Boron Nitride Is an Indirect Bandgap Semiconductor. *Nat. Photonics* **2016,** *10,* 262-266.
36. Ramasubramaniam, A.; Naveh, D.; Towe, E. Tunable Band Gaps in Bilayer Graphene-BN Heterostructures. *Nano Lett.* **2011,** *11*, 1070-1075.

37. Song, X.; Sun, J.; Qi, Y.; Gao, T.; Zhang, Y.; Liu, Z. Graphene/*h*-BN Heterostructures: Recent Advances in Controllable Preparation and Functional Applications. *Adv. Energy Mater.* **2016,** *6*, 1600541.
38. Kennedy, C. E. Review of Mid-to High-Temperature Solar Selective Absorber Materials; NREL/TP-520-31267; OSTI: Oak Ridge, TN, 2002.